Simulation of Condensing Compressible Flows

Maximilian Wendenburg

Outline

- Physical Aspects
  - Transonic Flows and Experiments
  - Condensation Fundamentals
  - Practical Effects
- Modeling and Simulation
  - Equations, Solver, Boundary Conditions
- Results
  - Validation
  - Effects in Laval Nozzles, Turbines and Compressors

Schlieren Photography: Visualizing $\frac{\partial \rho}{\partial x}$

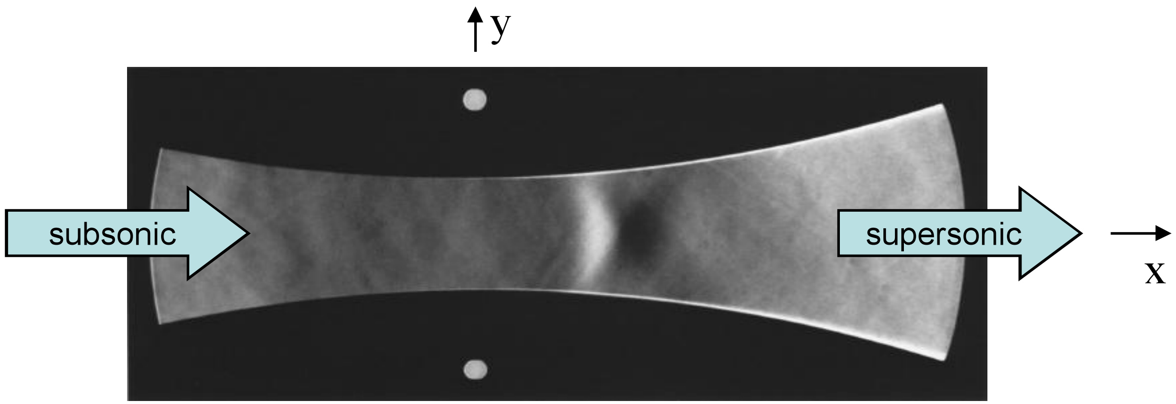

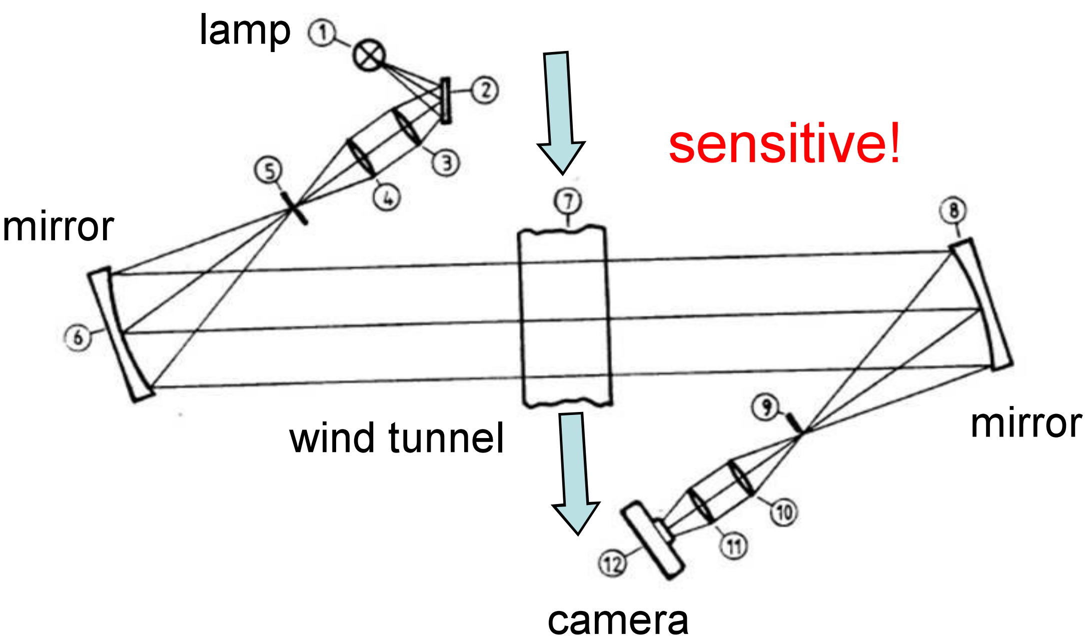

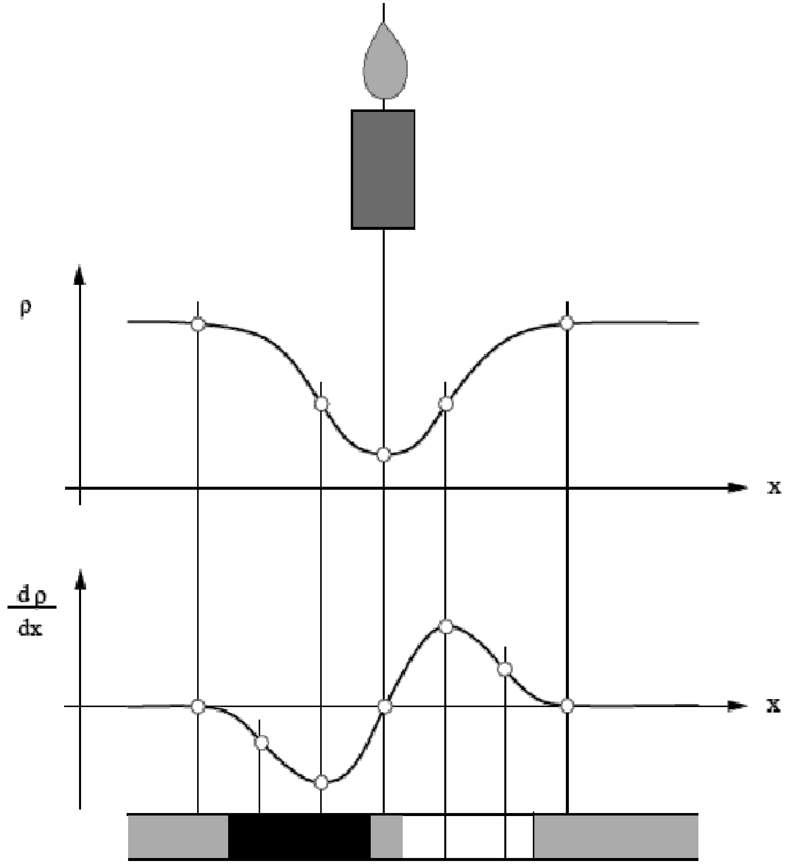

Supersonic Wind Tunnel

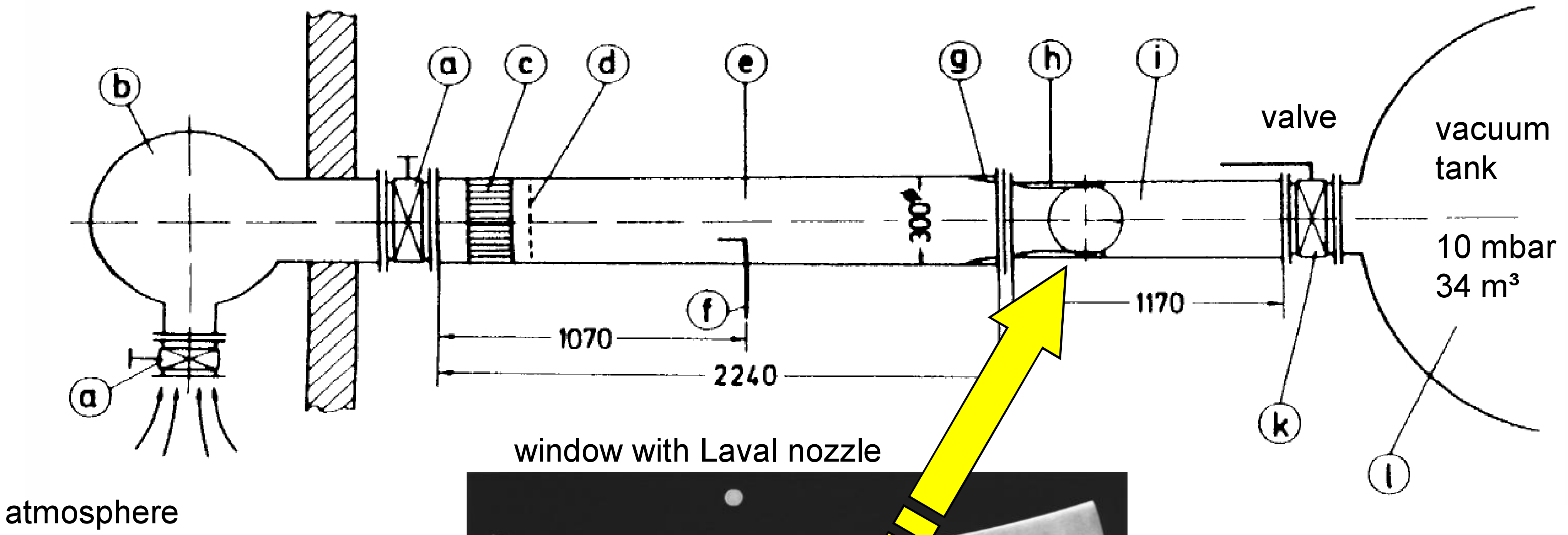

window with Laval nozzle

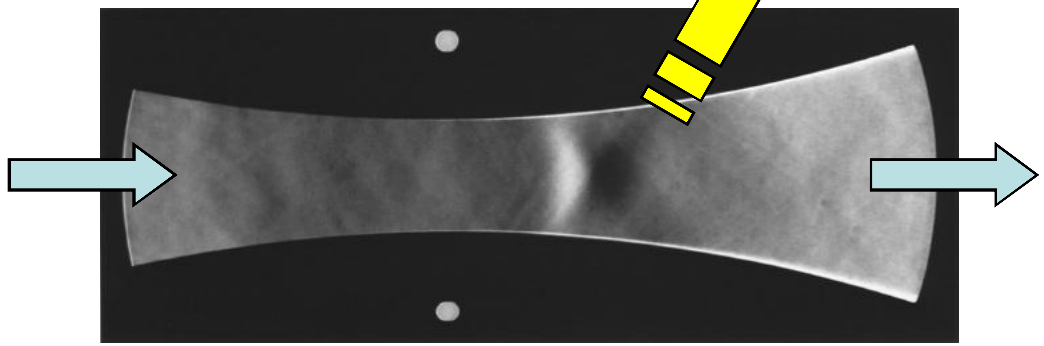

Variation of Static Properties in Isentropic Flows

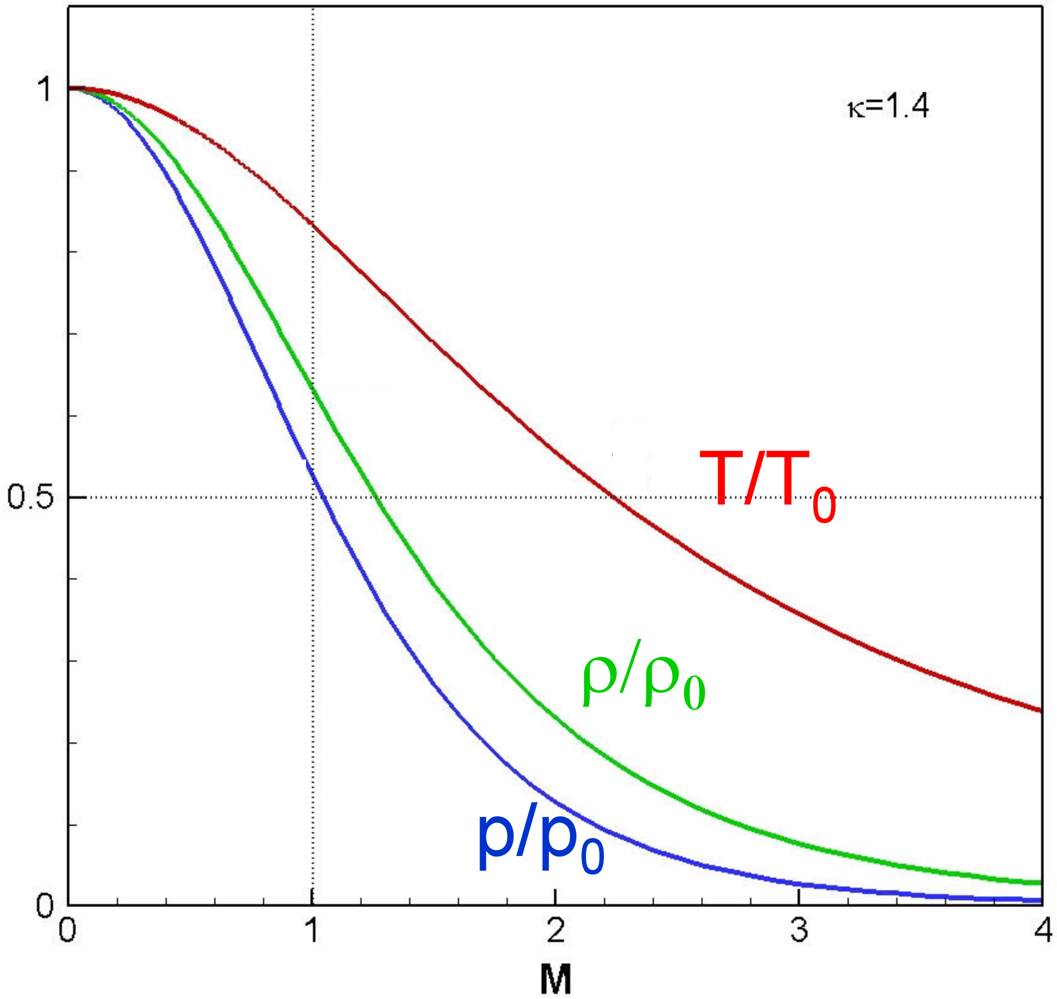

$$M = \frac{|\vec{u}|}{a}$$

Condensation of Dissolved Water Vapor in Air

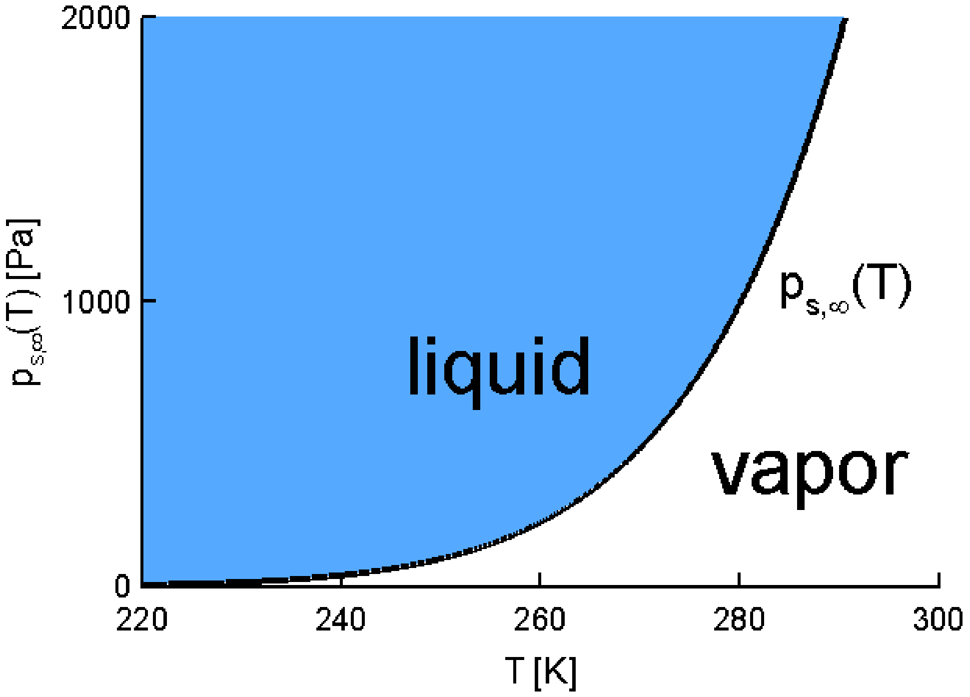



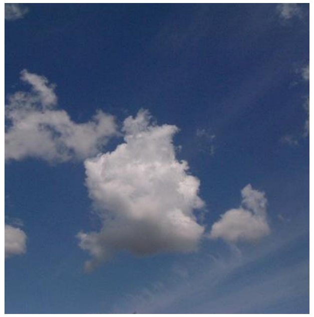

low cooling rate $\frac{dT}{dt} \approx -10^{-3} \frac{K}{s}$


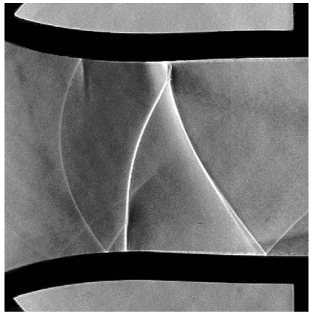


$\frac{dT}{dt} \approx -10^{5} \frac{K}{s}$ $\frac{dT}{dt} \approx -10^{6} \frac{K}{s}$

high cooling rate

Partial Pressure of Vapor p_v in Isentropic Expansion

$$S = \frac{p_v}{p_{s,\infty}(T)}$$

$$\Phi_0 = \frac{p_v}{p_{s,\infty}(T)} \cdot 100\%$$

Φ_0 = 65 %
T_0 = 295 K
$p_0 = 10^5$ Pa

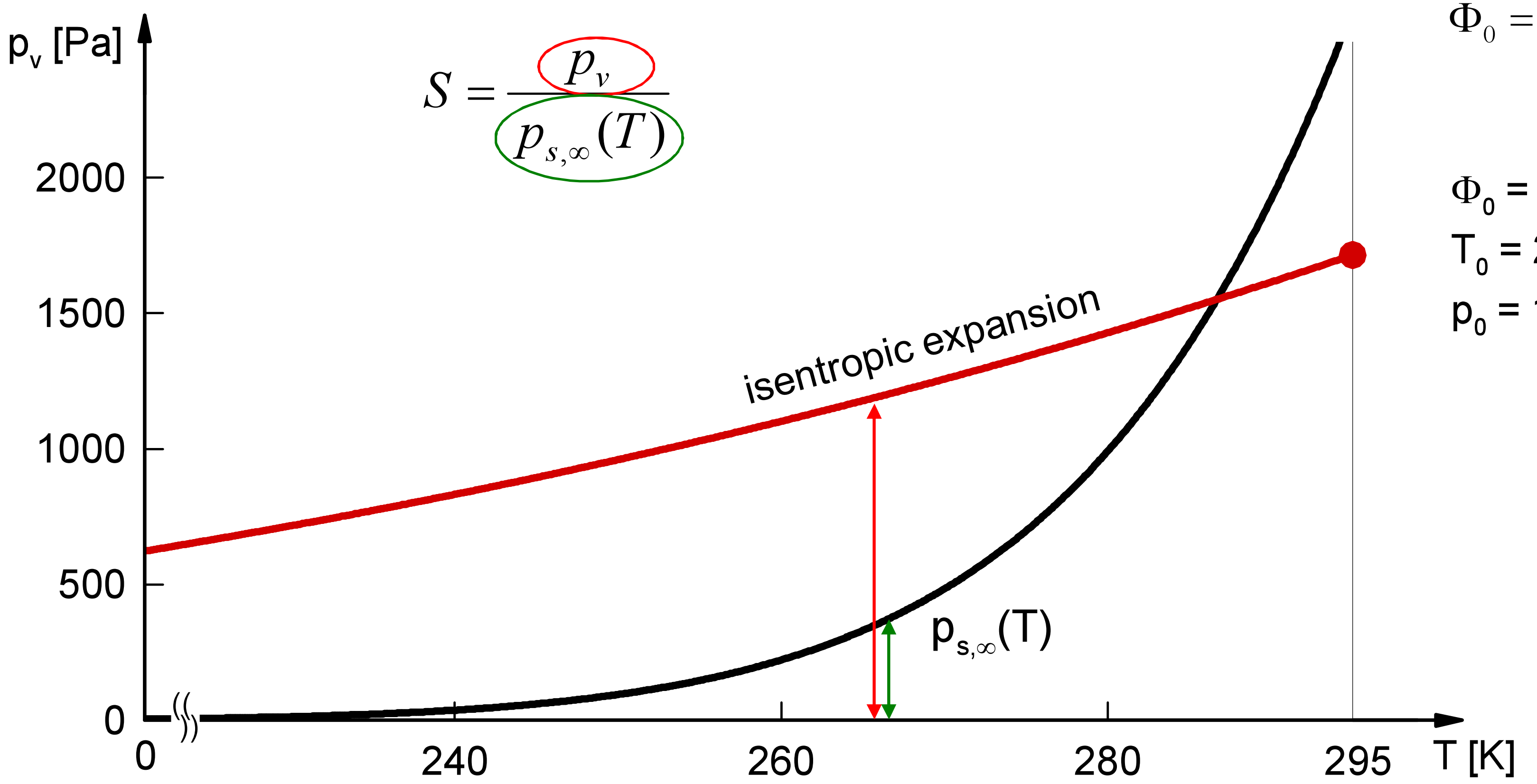

Types of Non-Equilibrium Condensation

Homogeneous

- Nucleation
  cluster → nucleus → droplet
- Droplet growth
- Dominates at high cooling rates

Heterogeneous

- Particles serve as seeds for droplets
- Dominates at low cooling rates

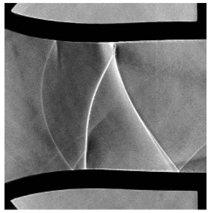

Practical Effects

- Aircraft
  - Influence on lift and drag
  - Loss of thrust
- Steam Turbines
  - Erosion
  - Oscillation

Physical Aspects

- Isentropic expansion: T↓, ρ↓, p↓
- Transonic flows

→High cooling rates ($\frac{dT}{dt} \approx -10^6 \frac{K}{s}$)

→Supersaturation → non-equilibrium

→Homogeneous/heterogeneous condensation

→Influence of condensation on flow

Euler Equations

$$\frac{\partial(\rho\phi)}{\partial t} + \nabla\cdot(\rho u\phi) = \rho\frac{D\phi}{Dt}$$

$$\frac{\partial\rho}{\partial t} + \nabla\cdot(\rho\vec{u}) = 0$$

$$\frac{\partial(\rho\vec{u})}{\partial t} + \nabla\cdot(\rho\vec{u}\otimes\vec{u} + p\underline{I}) = \vec{0}$$

$$\frac{\partial(\rho E)}{\partial t} + \nabla\cdot(\rho E\vec{u} + p\vec{u}) = 0$$

Thermodynamics, EOS:

$$e = E - \tfrac{1}{2}\vec{u}^2$$

$$T = T(e)$$

$$p = p(\rho, T)$$

$$a = \sqrt{\kappa R T}$$

Equations for Homogeneous Condensation

$$\frac{\partial(\rho n_{\text{hom}})}{\partial t} + \nabla \cdot (\rho n_{\text{hom}} \vec{u}) = J_{\text{hom}}$$

n	kg^{-1}	number density of droplets
g	-	condensate mass fraction
J	$m^{-3}\ s^{-1}$	nucleation rate

$$\frac{\partial(\rho g_{\text{hom}})}{\partial t} + \nabla \cdot (\rho g_{\text{hom}} \vec{u}) = \left(\underbrace{\rho_l \frac{4\pi}{3} r^{*3} J_{\text{hom}}}_{\text{nucleation}} + \underbrace{\rho_l 4\pi \bar{r}_{\text{hom}}^2 \rho n_{\text{hom}} \frac{d\bar{r}_{\text{hom}}}{dt}}_{\text{droplet growth}} \right)$$

$$J_{\text{hom}} = \sqrt{\frac{2}{\pi} \cdot \frac{\sigma_\infty(T)}{m_v^3}} \cdot \frac{\rho_v^2}{\rho_l} \cdot \exp\left(-\frac{4\pi}{3} \cdot \frac{r_{\text{hom}}^{*2} \cdot \sigma_\infty(T)}{m_v \cdot R_v \cdot T} \right)$$

$$g = \frac{m_l}{\underbrace{m_a + m_v + m_l}_{\text{total masses}}}$$

$$\bar{r}_{\text{hom}} = \sqrt[3]{\frac{3}{4\pi} \cdot \frac{g}{\rho_l \cdot n_{\text{hom}}}}$$

$$\frac{d\bar{r}_{\text{hom}}}{dt} = \frac{\alpha}{\rho_l} \cdot \frac{p_v - p_{s,r}}{\sqrt{2\pi \cdot R_v \cdot T}}$$

Hertz-Knudsen Law

Multiphase-Multicomponent Thermodynamics

$$e = E - \tfrac{1}{2}\vec{u}^2$$

$$T = T(e, g_{\max}, g)$$

$$p = p(\rho, T, g_{\max}, g)$$

$$\kappa = \kappa(g_{\max}, g, T)$$

$$a = \sqrt{\kappa \tfrac{p}{\rho}}$$

- Air as carrier gas with vapor:
  both ideal gases

- Pure water vapor:
  real gas behavior

Solver

- CATUM
  - **C**ondens**a**tion **T**echnische **U**niversität **M**ünchen
  - density-based FVM solver
    - Cell-averaged values
    - Considering fluxes over cell boundaries: conservative
  - 1-D, 2-D, 3-D
  - on structured multiblock grids
  - approach: solve local Riemann problems

Finite Volume Method

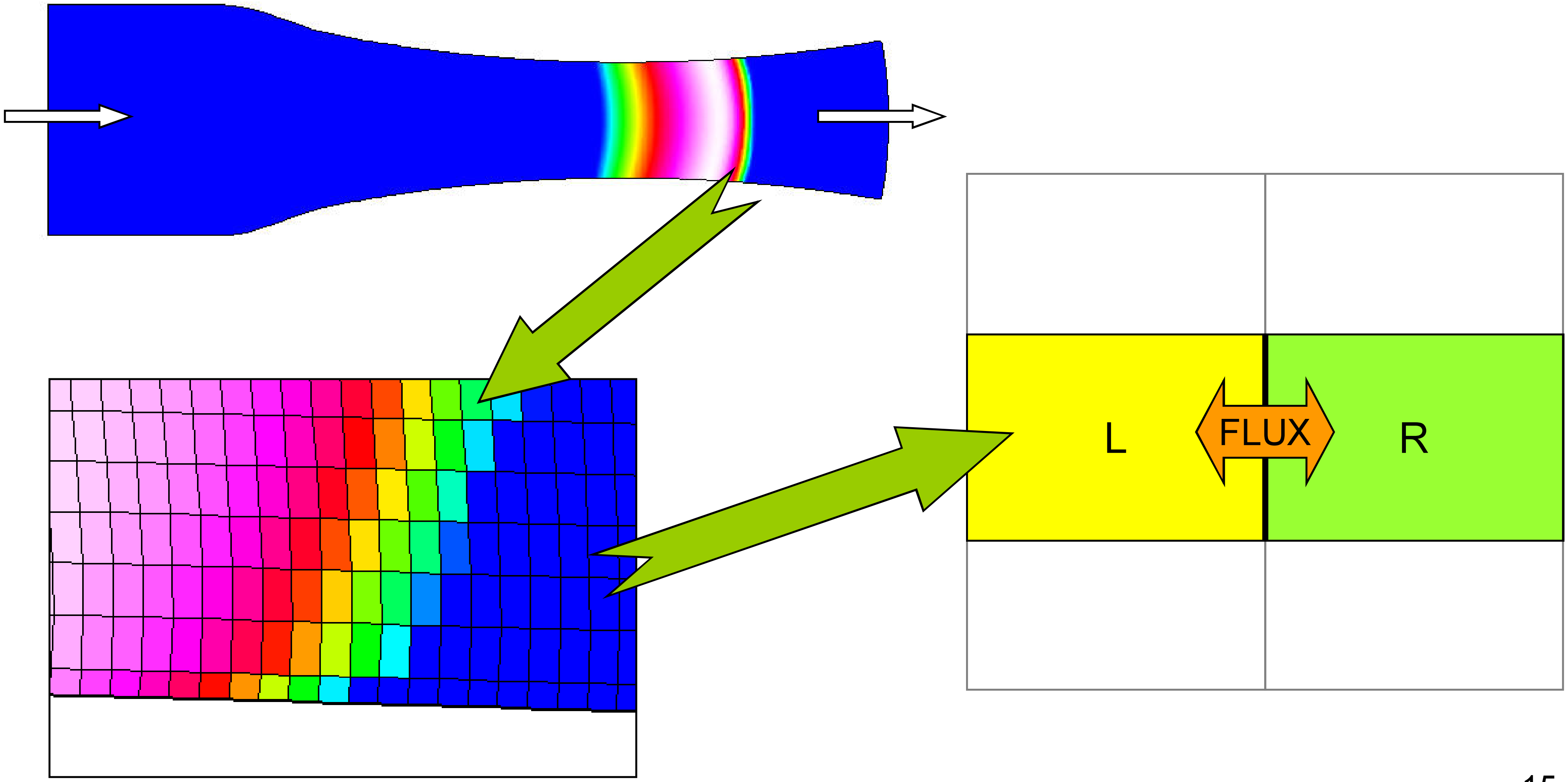

Reconstruction at Cell Faces

- Average values stored in cell center
- Reconstruct the required value at the cell face
- 4 adjacent cells for 2nd order accuracy
- Limiter functions: high order smoothness where continuous, low order sharpness at shocks

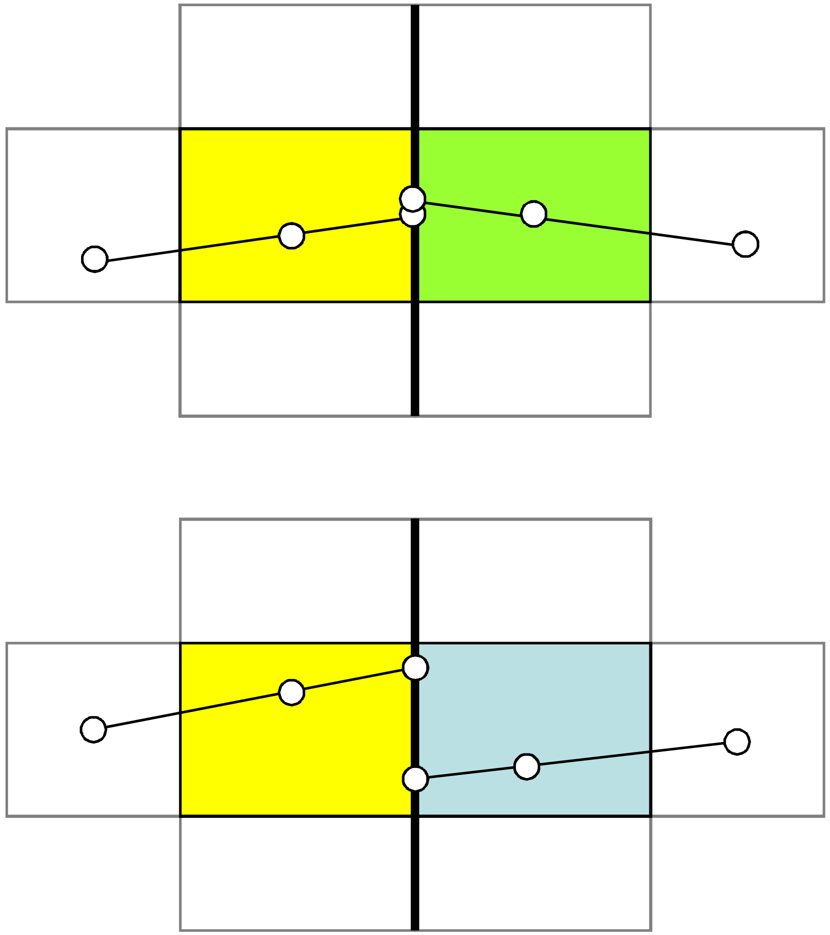

1-D Riemann Problem

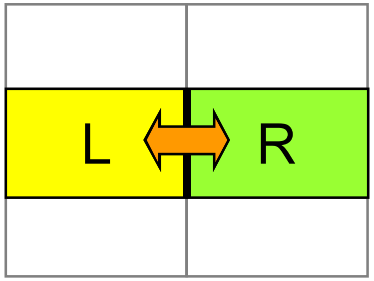

$$Q_t + F(Q)_x = 0 \qquad Q = \begin{pmatrix} \rho \\ \rho u \\ \rho E \end{pmatrix} \qquad F(Q) = \rho u \begin{pmatrix} 1 \\ u \\ E \end{pmatrix} + \begin{pmatrix} 0 \\ p \\ up \end{pmatrix}$$

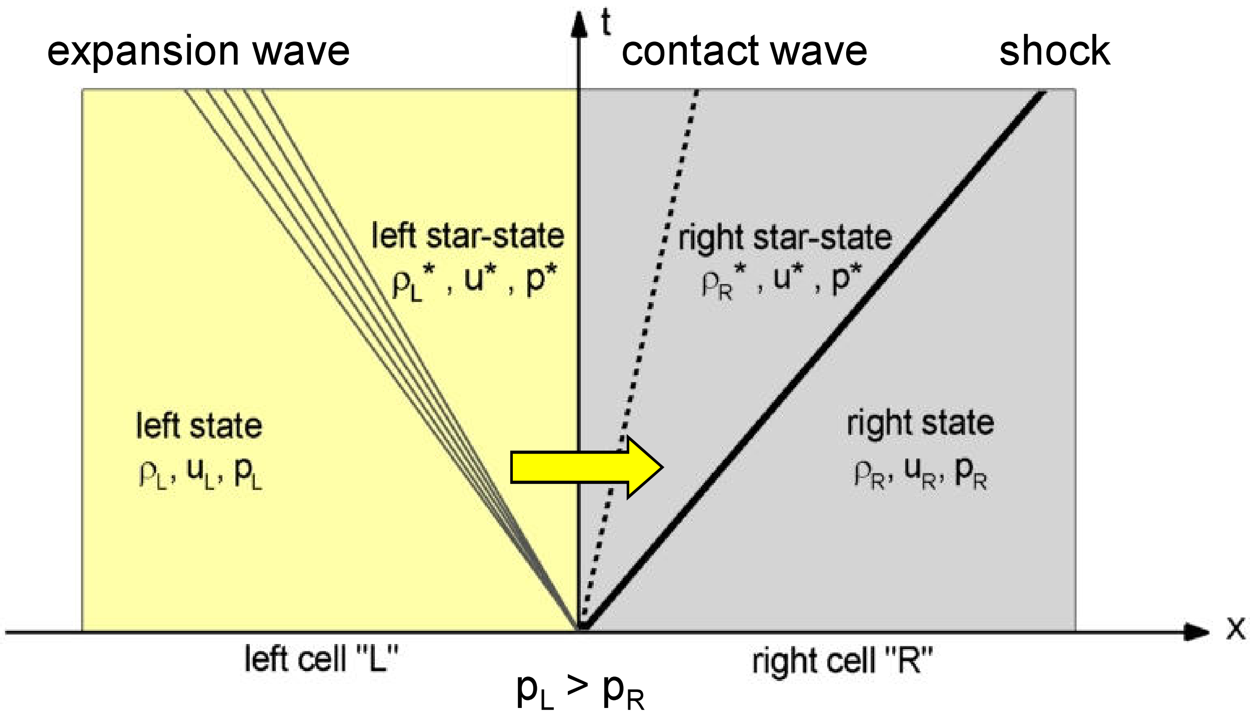

Boundary Conditions: “Ghost Cells”

- General: 2 “ghost cells” for 2nd order accuracy
- Inlet
  - Pressure extrapolated from outermost cell, other values calculated from stagnation conditions (p_0, T_0, …) by isentropic relationships, e.g. with

$$\frac{p_1}{p_2} = \left(\frac{1 + \frac{\kappa - 1}{2} M_2^2}{1 + \frac{\kappa - 1}{2} M_1^2} \right)^{\frac{\kappa}{\kappa - 1}}$$

- Wall
  - Velocity normal to wall is zero

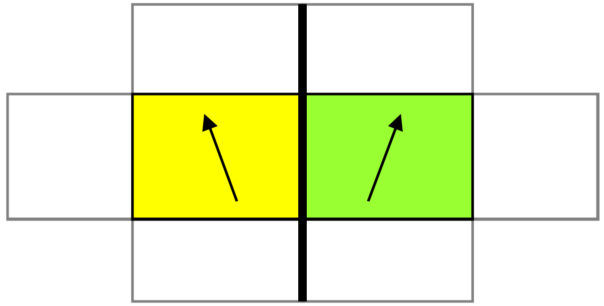

- Outlet
  - Subsonic: set outlet pressure, extrapolate other values
  - Supersonic: extrapolate all

Modeling and Simulation

- Euler equations
- Additional Eqns. for Condensation
  - Influence on EOS
- Reconstruction
- Riemann problem
- BCs via ghost cells

Validation of the Implementation

Nozzle S2

T_0 = 300 K

$p_0 = 10^5$ Pa

Φ_0 = 35.3 %

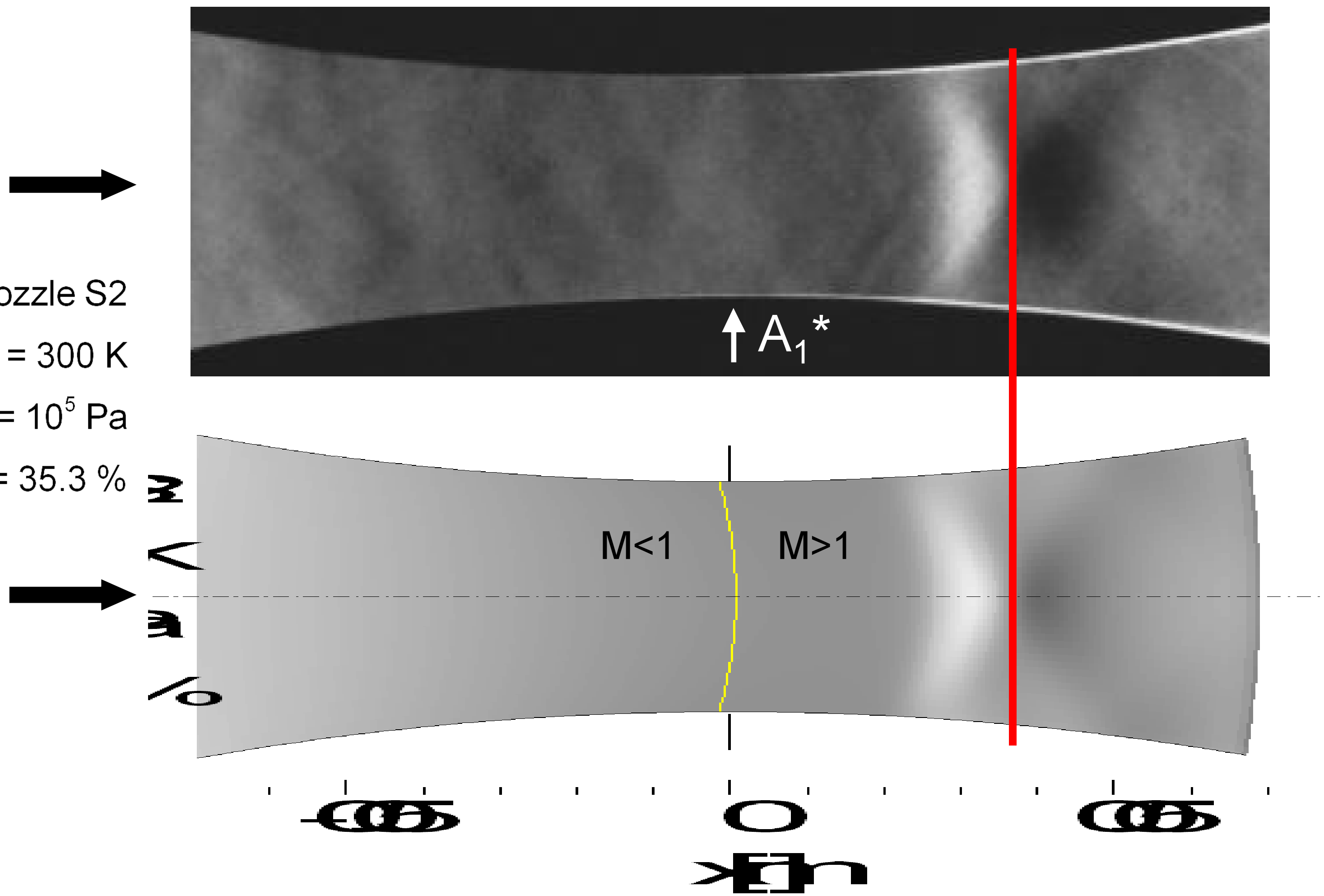

Subcritical Heat Addition in Nozzle S2

Nozzle S2

T_0 = 300 K

$p_0 = 10^5$ Pa

Φ_0 = 35.3 %

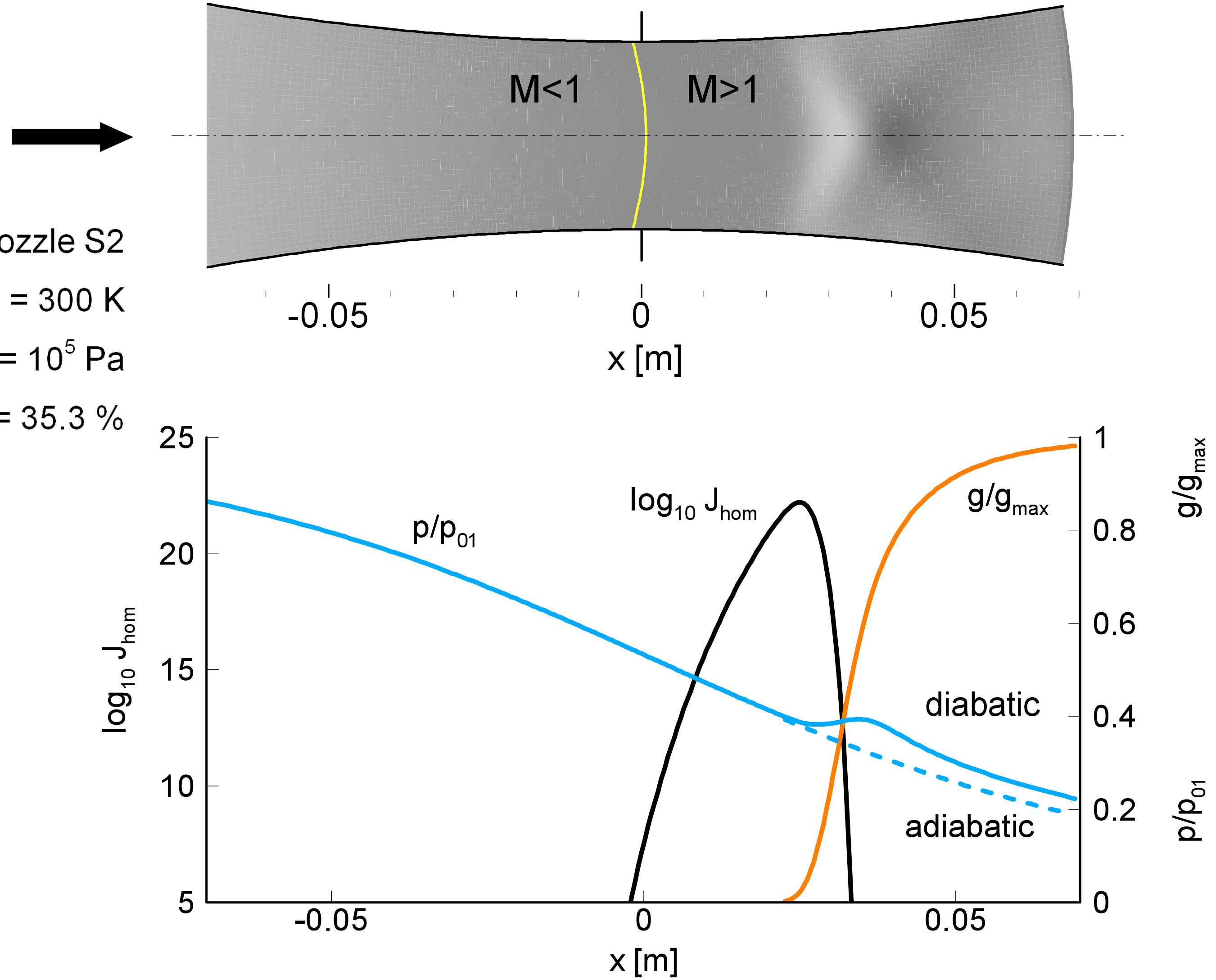

Supercritical Heat Addition in Nozzle S2

Nozzle S2

T_0 = 295 K

$p_0 = 10^5$ Pa

Φ_0 = 65 %

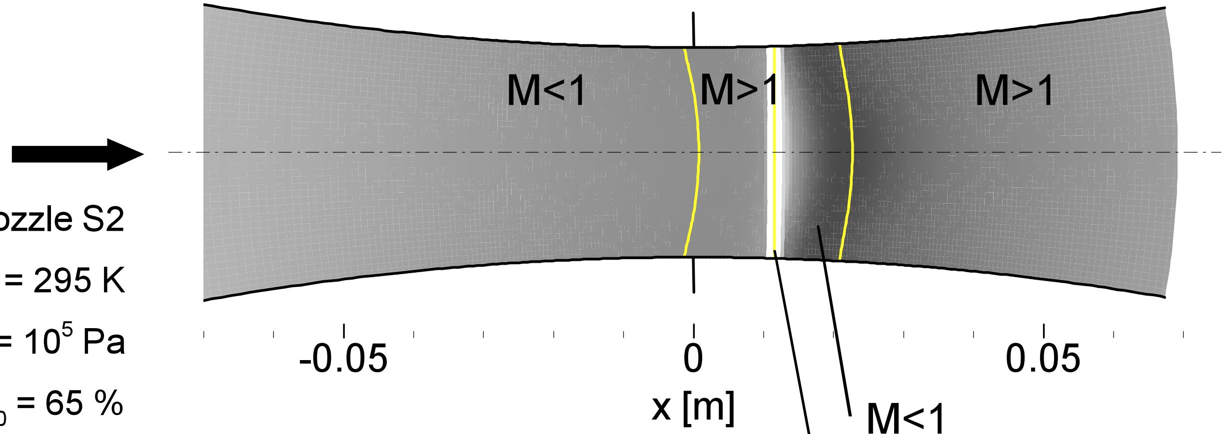

shock: increase of T, ρ, p

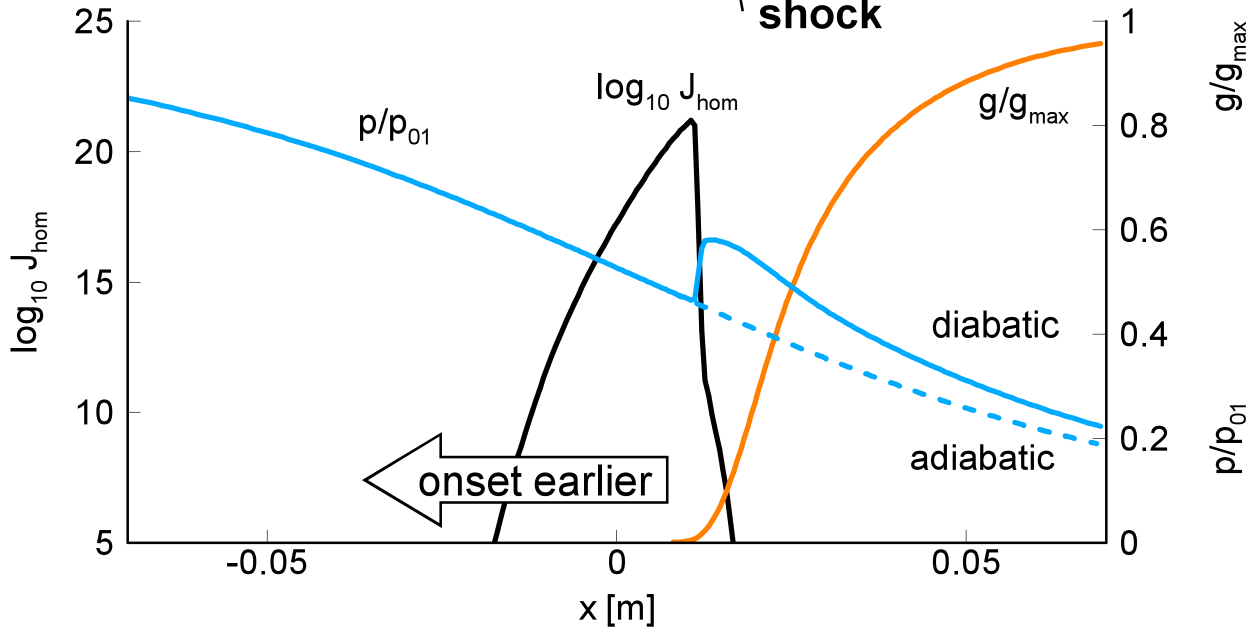

Condensing Flows in Nozzle S2

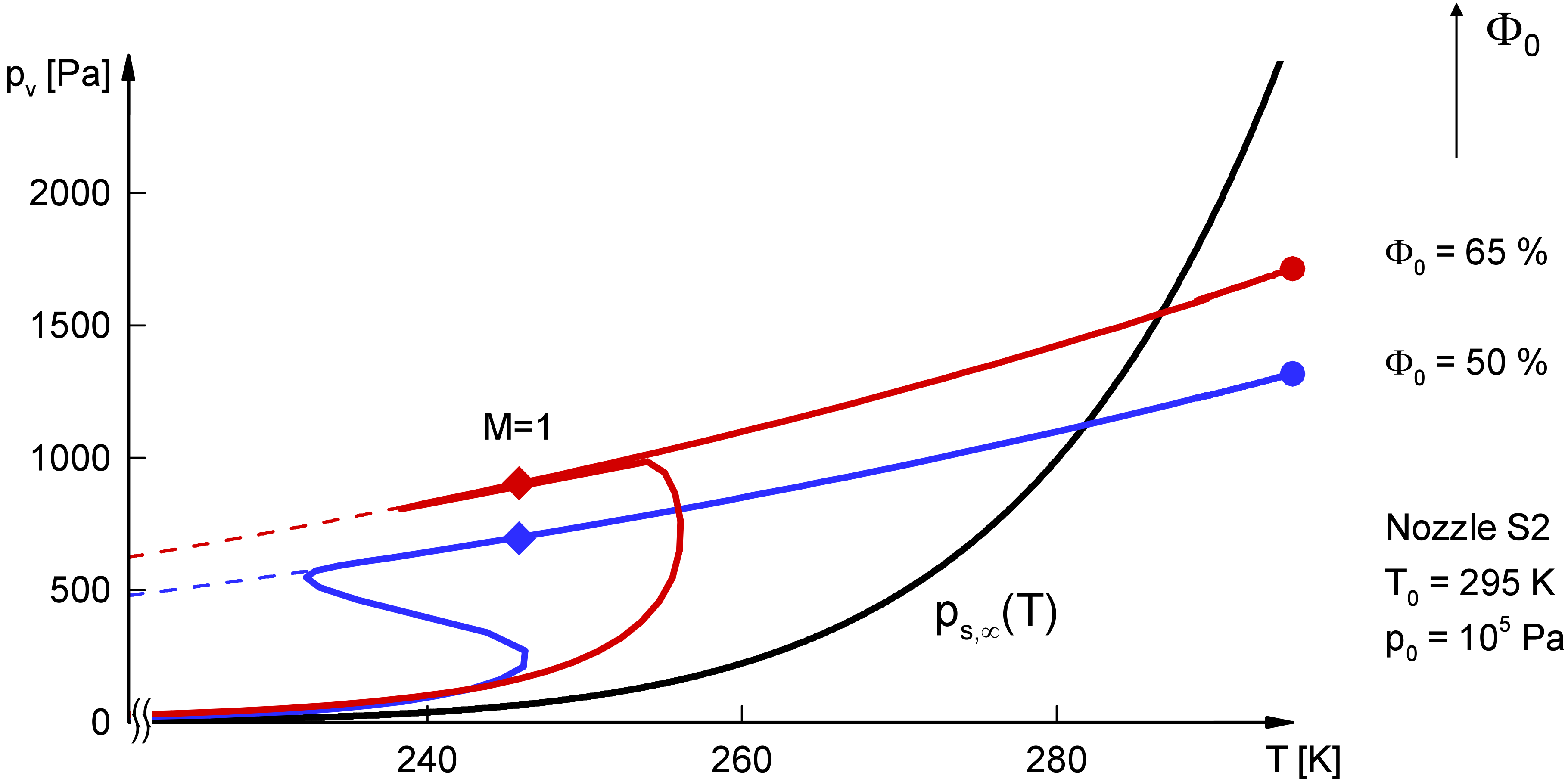

Unsteady Effects at High Relative Humidity

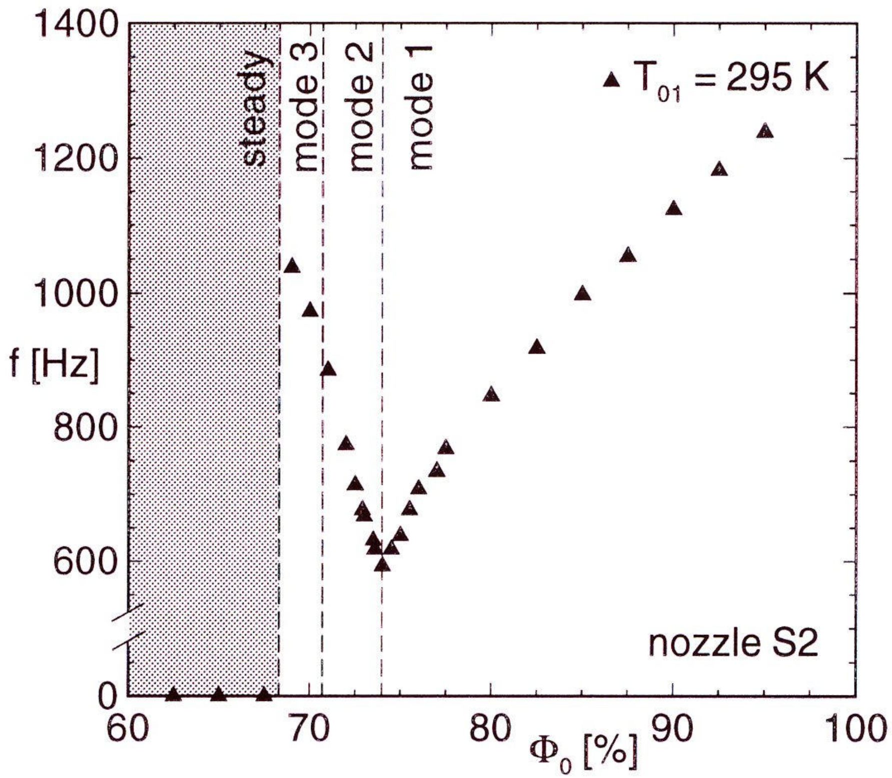

Validation of the Implementation

- T_0 = 291.7 K
- p_0 = 1.006 x 10^5 Pa
- Φ_0 = 91.1 %
- Mode 1

- f = 948 Hz
- ½ grid: 241x21 cells

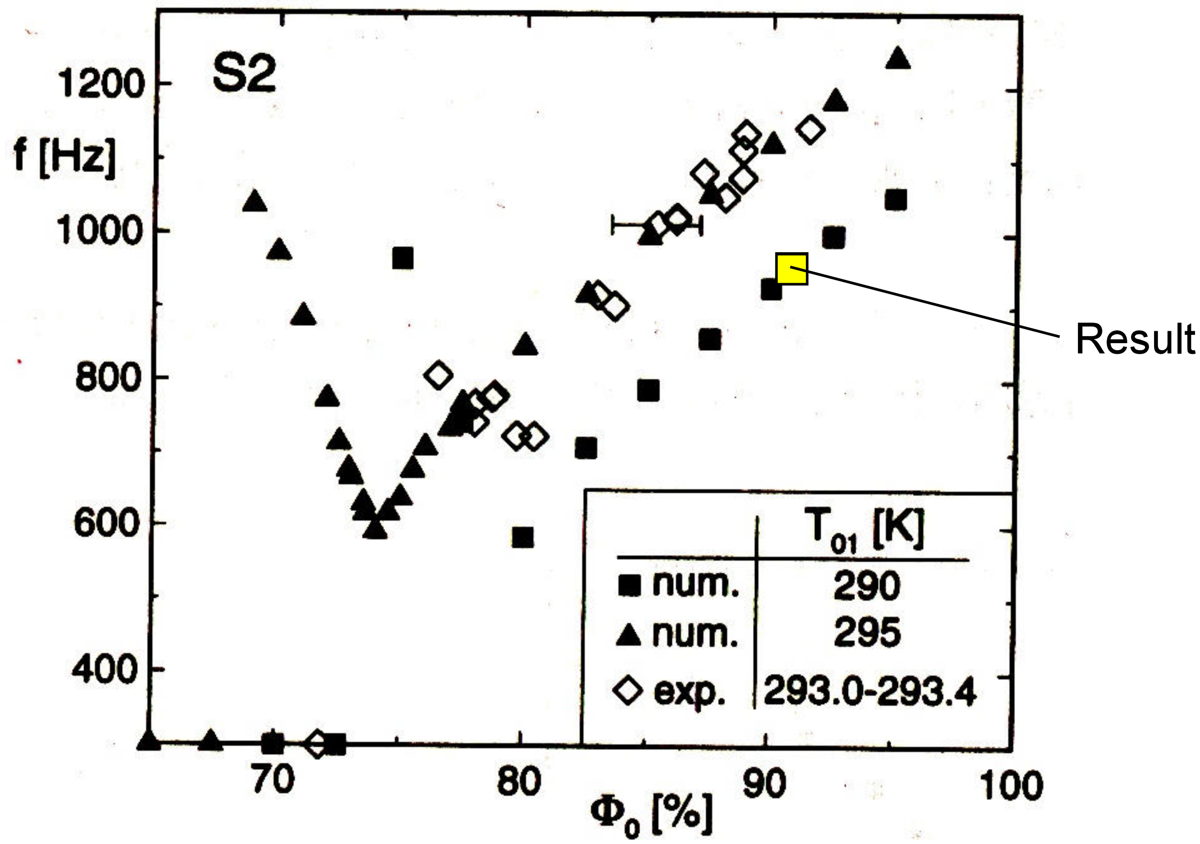

Symmetric Oscillation in Nozzle S2

- T_0 = 291.7 K
- p_0 = 1.006 x 10^5 Pa
- Φ_0 = 91.1 %
- Mode 1
- f = 948 Hz
- ½ grid: 241x21 cells

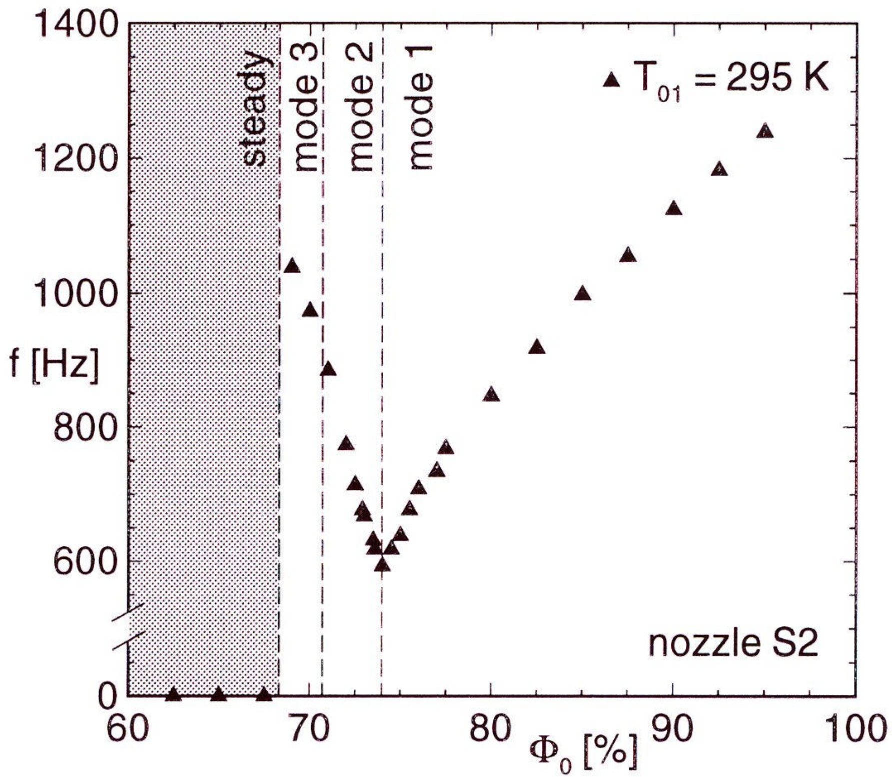

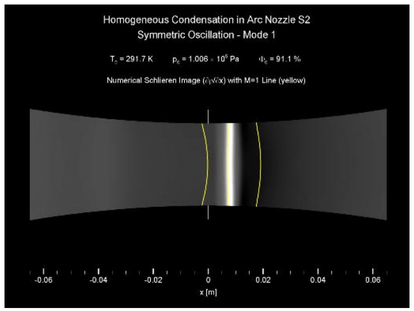

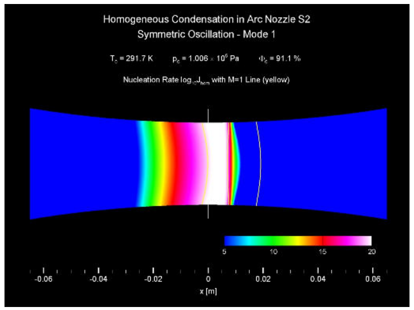

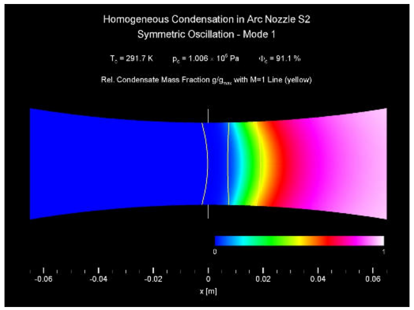

Hysteresis in Nozzle A1

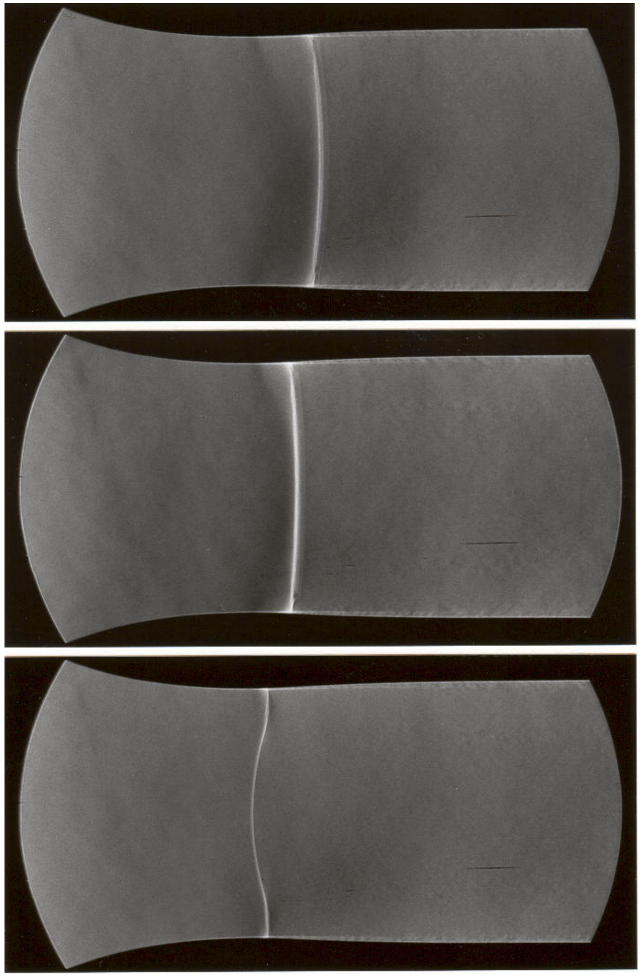

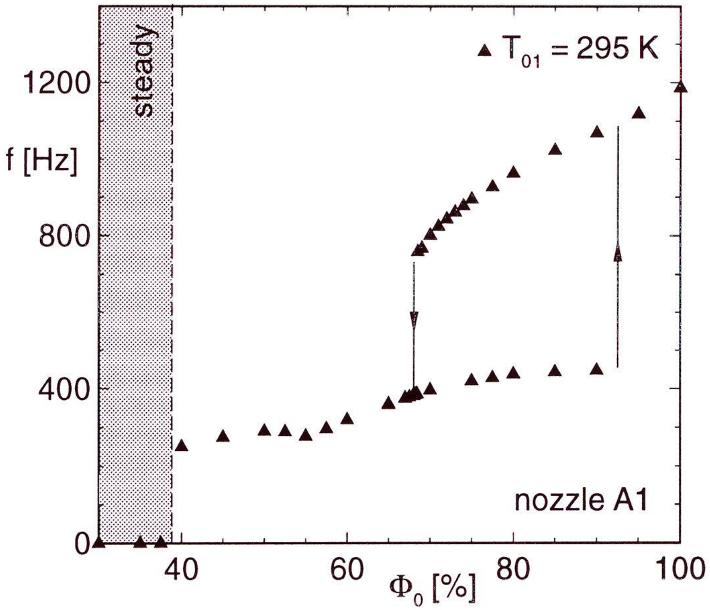

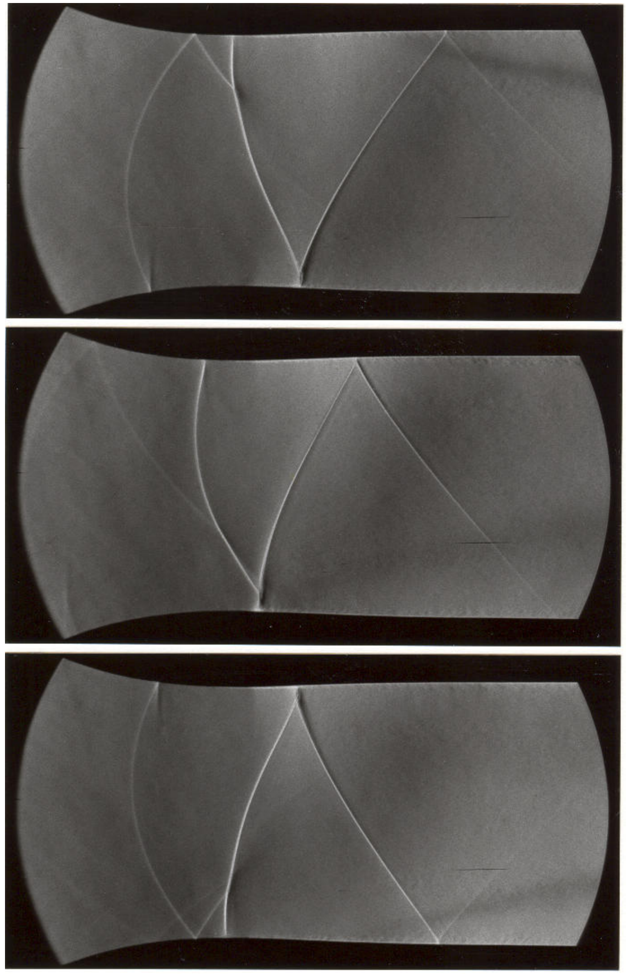

Flow in Nozzle A1

- T_0 = 305 K
- $p_0 = 10^5$ Pa
- Φ_0 = 77 %

- f = 1082 Hz
- full grid: 220 x 41

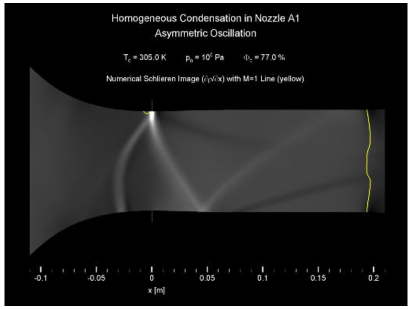

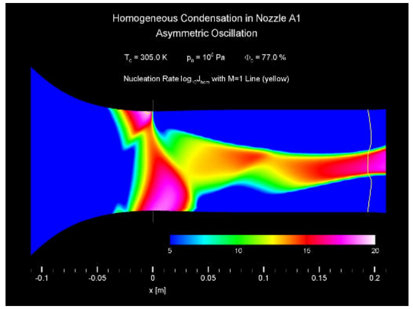

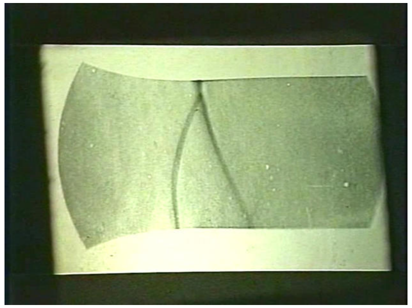

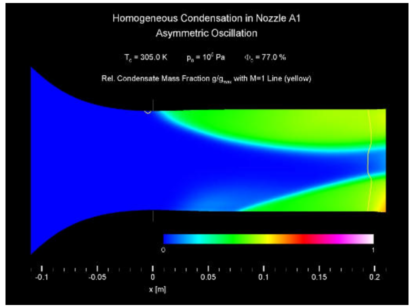

Asymmetric Oscillation in Nozzle S2

- T_0 = 305 K
- $p_0 = 10^5$ Pa
- Φ_0 = 95 %

- f = 3073 Hz
- full grid: 241x41 cells

enforced disturbance

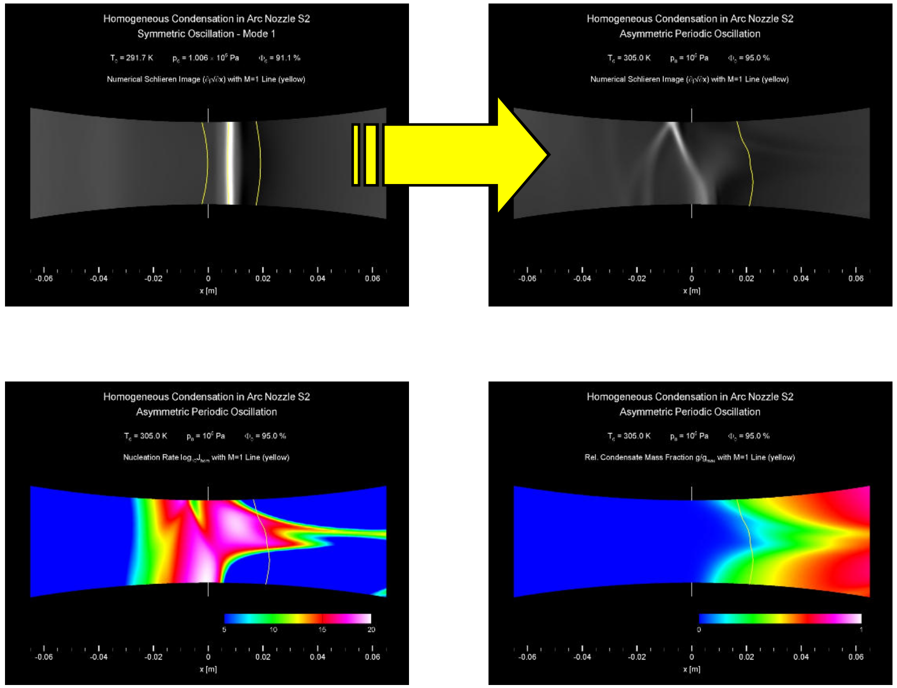

Turbine Stage VKI

with viscous effects

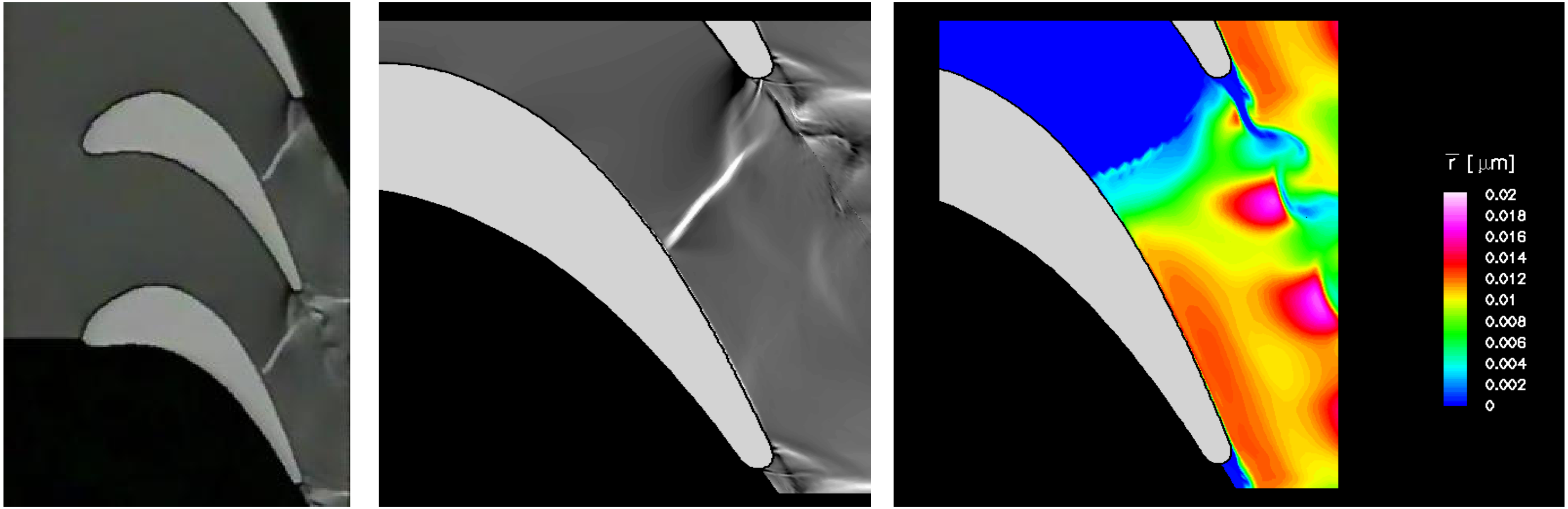

Rotor Stator Interaction

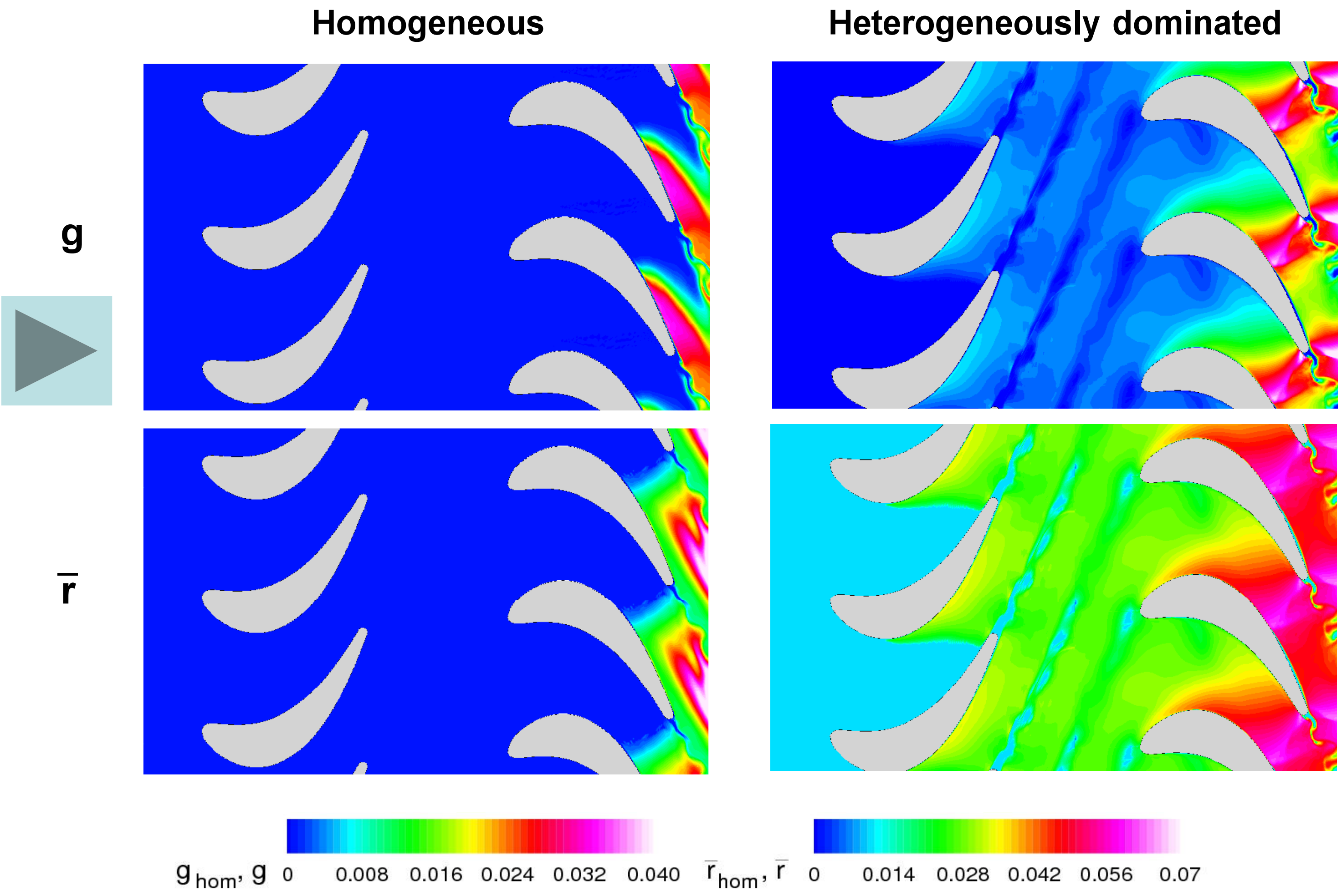

- p_{01} = 0.417 bar
- T_{01} = 357.5 K
- $\beta_{1,1}$ = 120°
- $Re_{rotor} = 1.13 \cdot 10^{6}$
- $M_{2,2,is}$ = 1.13
- $|u|$ = 175 m/s
- $n_{het,0} = 10^{16}\ m^{-3}$
- $r_{het} = 10^{-8}$ m
- f_{rs} = 2.46 kHz
- $f_{vs,stator}$ = 10.8 kHz
- $f_{vs,rotor}$ = 18.5 kHz

Supersonic Axial Compressor

NORD-1500 Griffon II (1957)
M_{max}=2.2, H_{max}=16400m, 34.32 kN

Alpha Jet (1973)
M_{max}=0.85, H_{max}=14630m, 14.12 kN

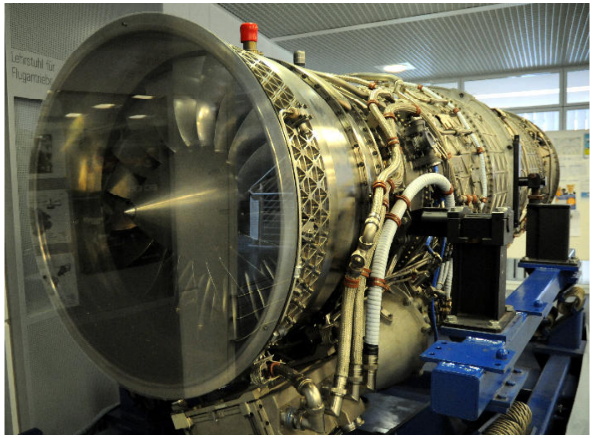

First Stage of a Supersonic Axial Compressor

Developed view of
a cylindrical cut

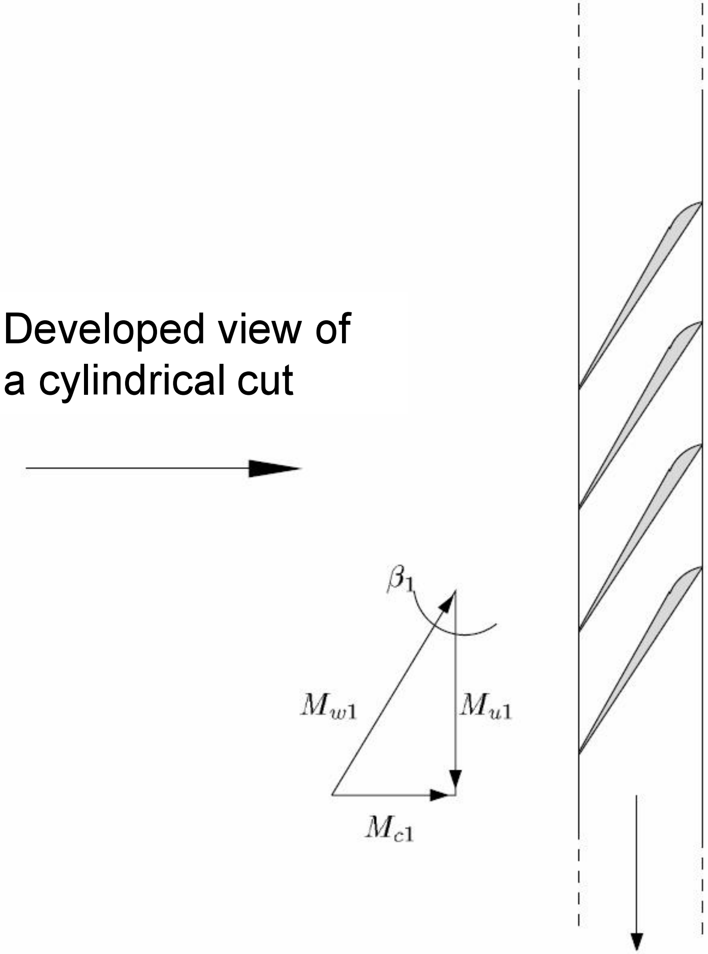

Section of Axial Compressor Stage

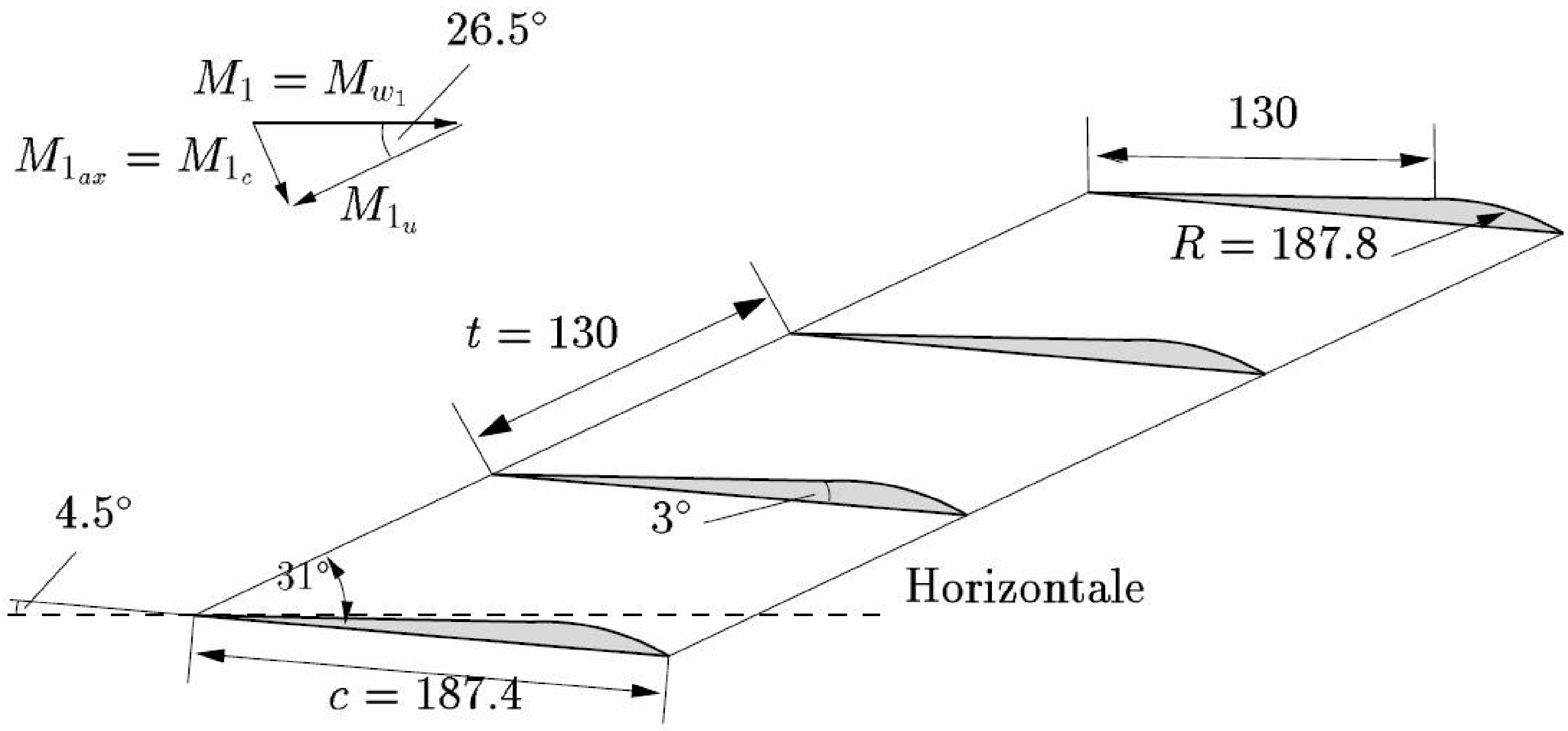

Cascade Element

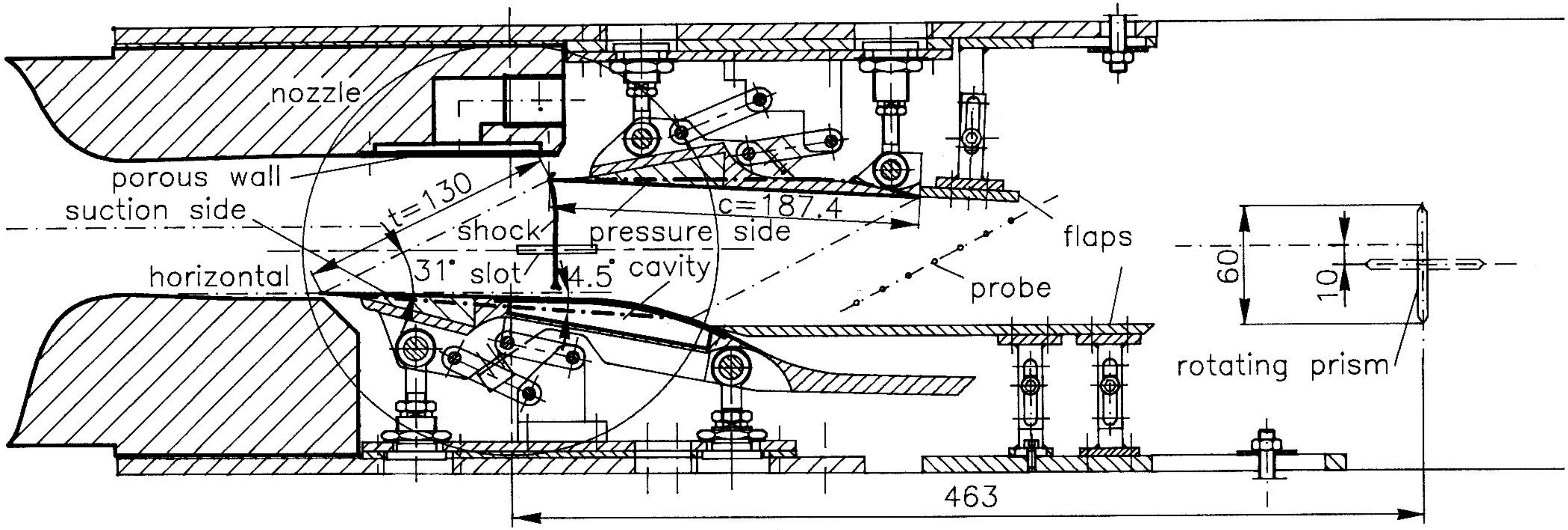

Experimental Setup

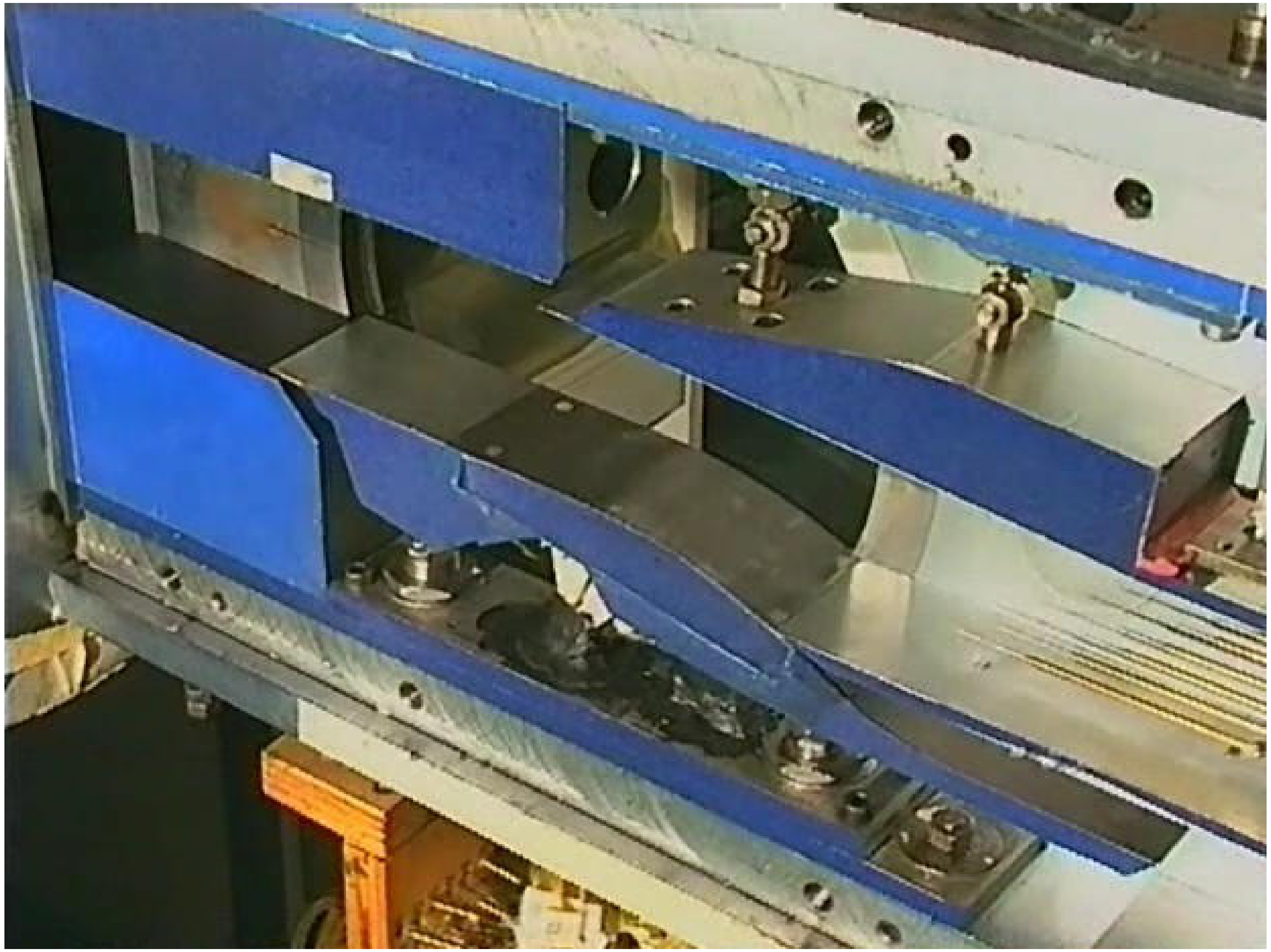

Cascade Element of an Axial Transonic Compressor

M_1=1.3 →

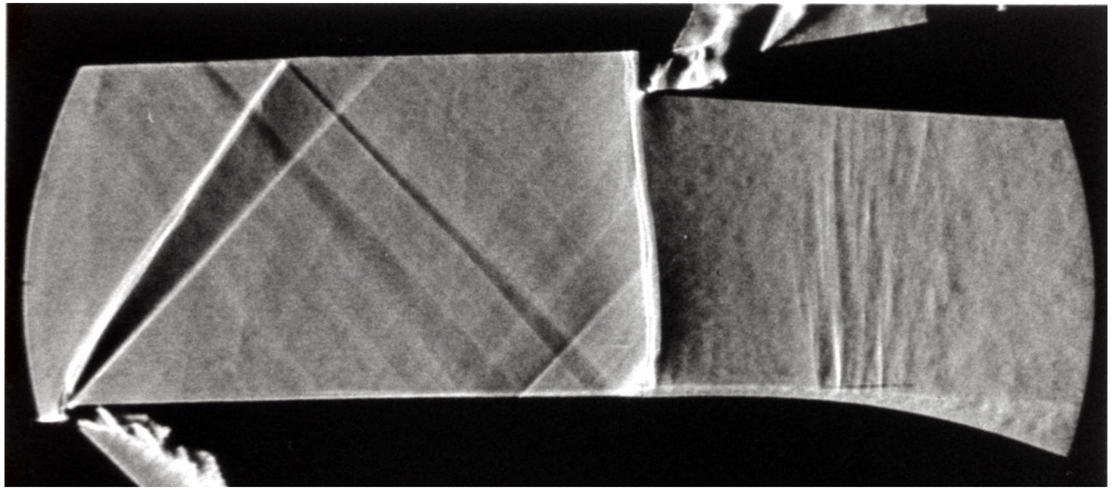

$\pi = p_2/p_1 = 1.764$

adiabatic flow

$$\frac{\pi_{\text{diabatic}}}{\pi_{\text{adiabatic}}} = 0.816$$

reduction of ca. 18%

→

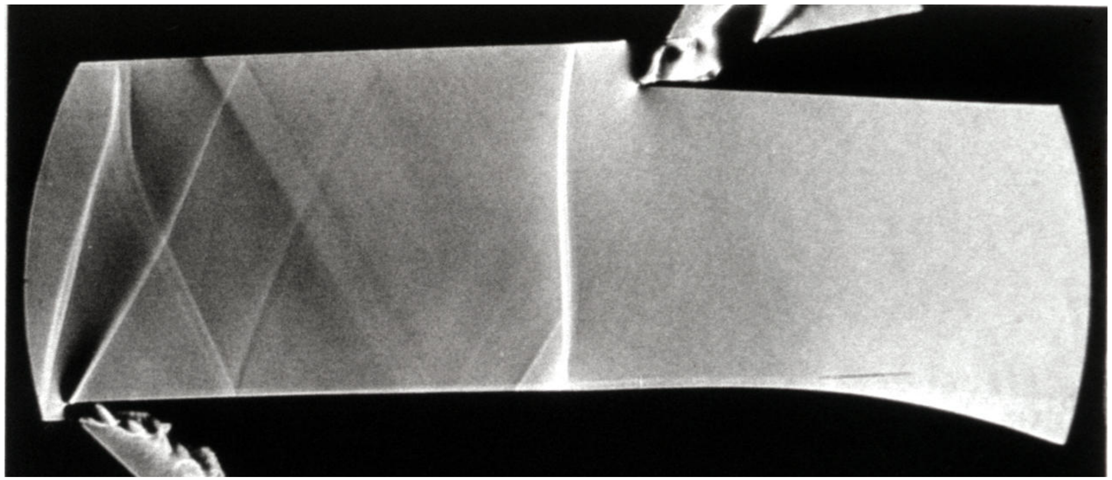

$\pi = p_2/p_1 = 1.440$

diabatic flow

T_{01}=291 K
p_{01}=1.008 bar
ϕ_0=80 %
x=10 g/kg

Cascade Element of an Axial Transonic Compressor

$M_1=1.3$ →

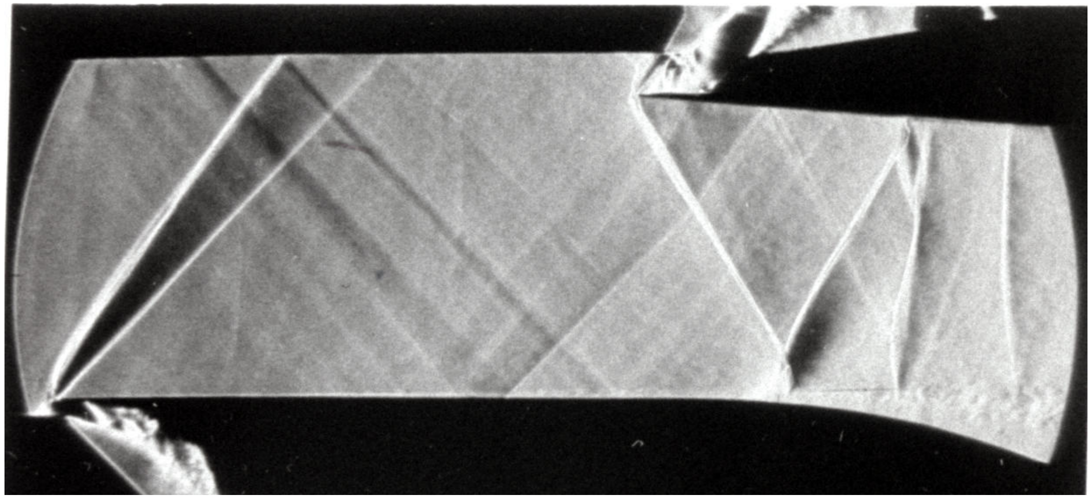

$\pi=p_2/p_1=1.630$

adiabatic flow

$$\frac{\pi_{diabatic}}{\pi_{adiabatic}} = 0.833$$

reduction of ca. 17%

→

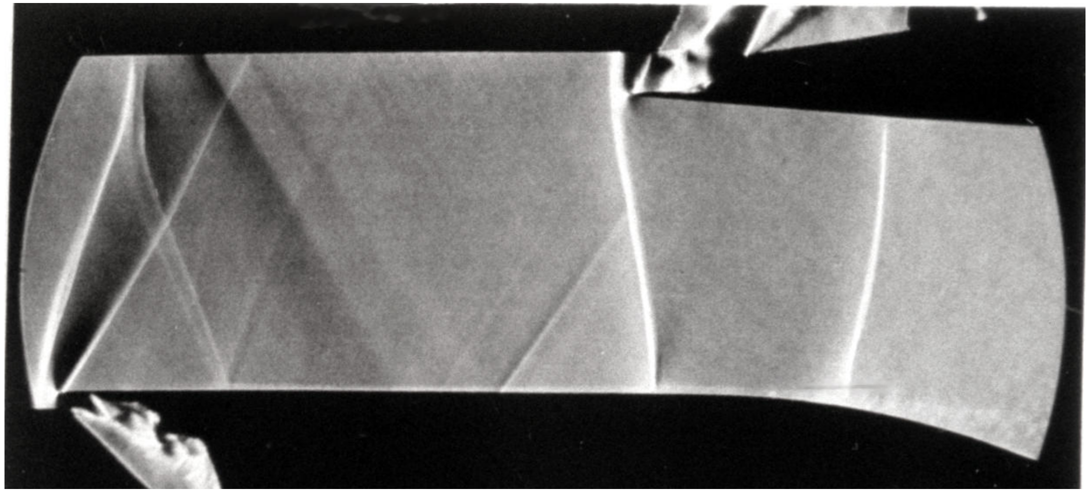

$\pi=p_2/p_1=1.358$

diabatic flow

$T_{01}=292$ K
$p_{01}=1.006$ bar
$\phi_0=69.8$ %
x=9.6 g/kg

Cascade Element of an Axial Transonic Compressor

M_1=1.3 →

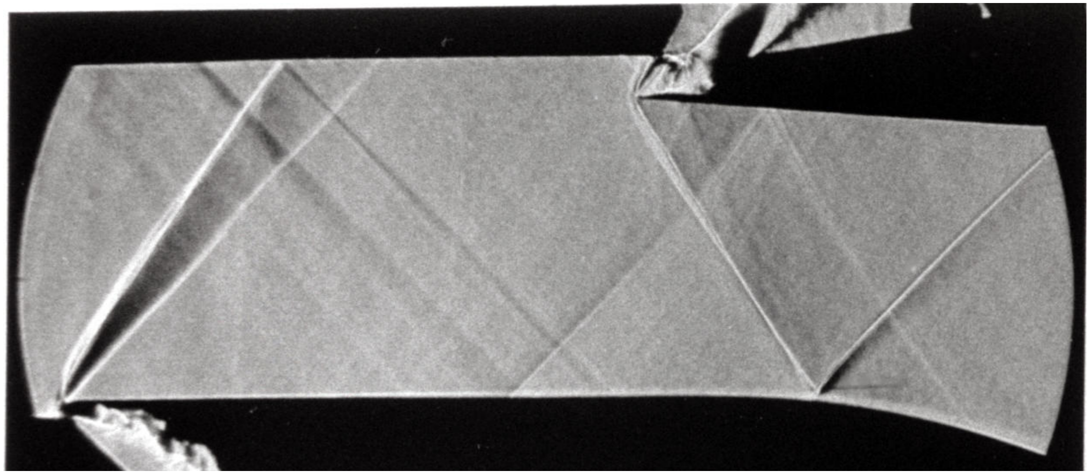

$\pi=p_2/p_1=1.055$

adiabatic flow

$$\frac{\pi_{diabatic}}{\pi_{adiabatic}} = 0.844$$

reduction of ca. 15%

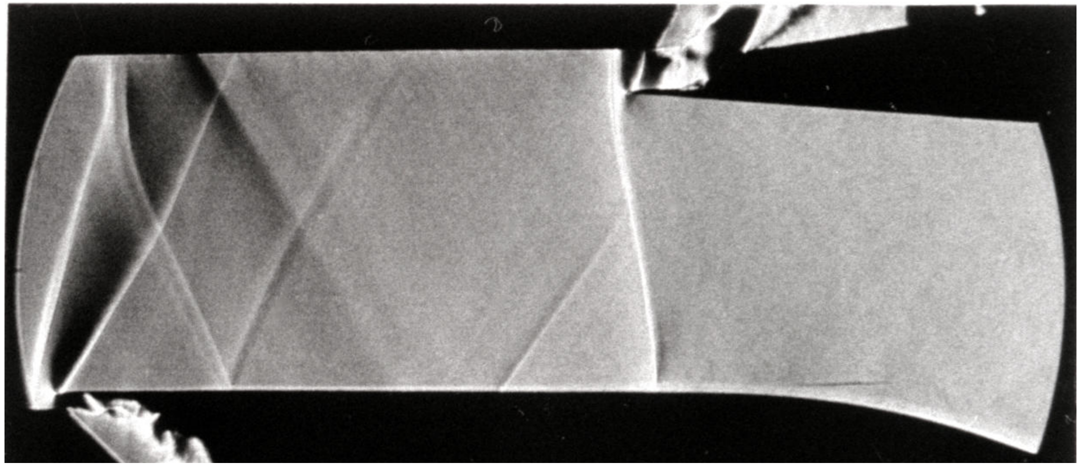

$\pi=p_2/p_1=0.890$

diabatic flow

T_{01}=294 K
p_{01}=1.005 bar
ϕ_0=80.3 %
x=9.6 g/kg

Condensation Effects in Transonic Compressors

- Reduction of
  - inlet Mach number
  - stage compression ratio
- Loss of
  - thrust
  - efficiency

Results

- Steady flows
  - Subcritical
  - Supercritical
- Unsteady flows
  - Symmetric/asymmetric oscillations
  - Different modes
- Effects in Turbomachinery

Спасибо

Thank you for your attention!

Discussion

Critical Radius

$$r^*_{\text{hom}} = \frac{2 \cdot \sigma_\infty(T)}{\rho_l(T) \cdot R_v \cdot T \cdot \ln(S)}$$

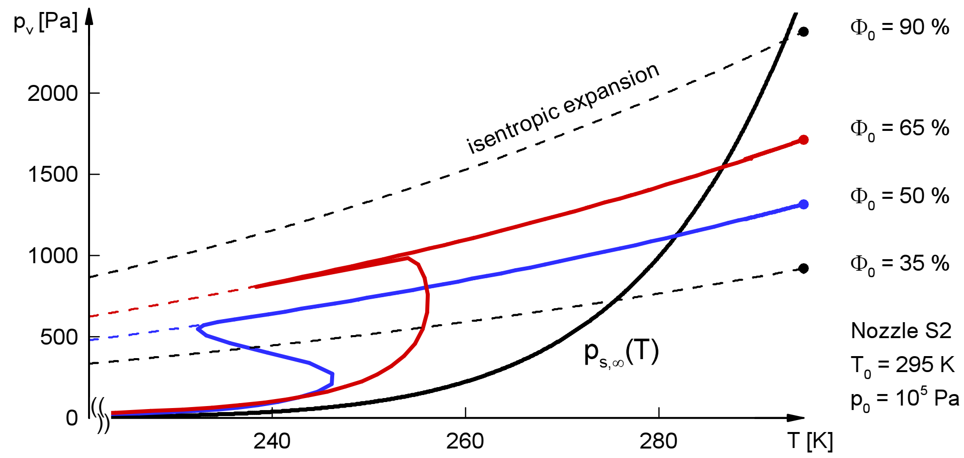

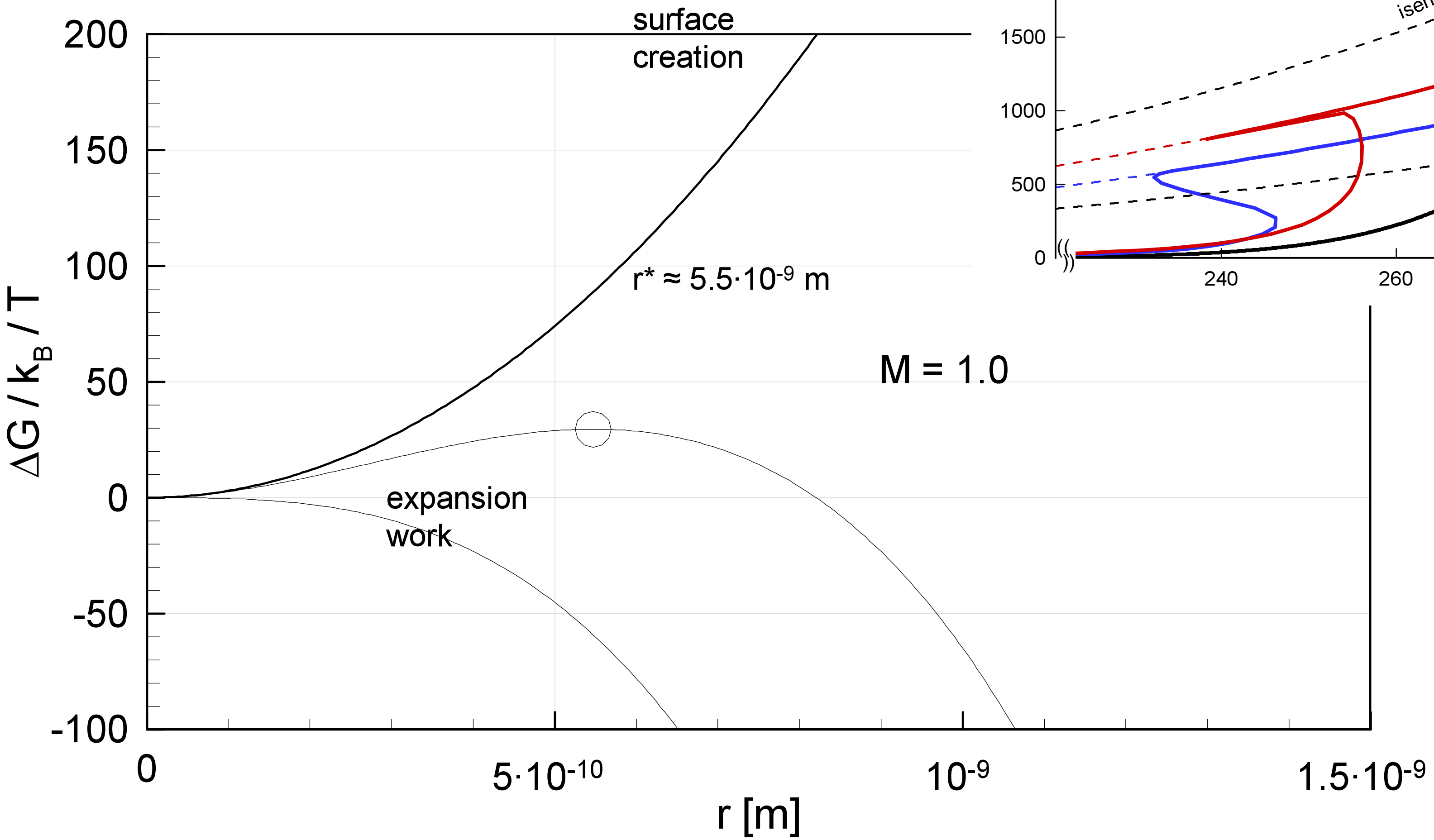

$T_0 = 295$ K

$p_0 = 10^5$ Pa

$\Phi_0 = 65$ %

Critical Radius

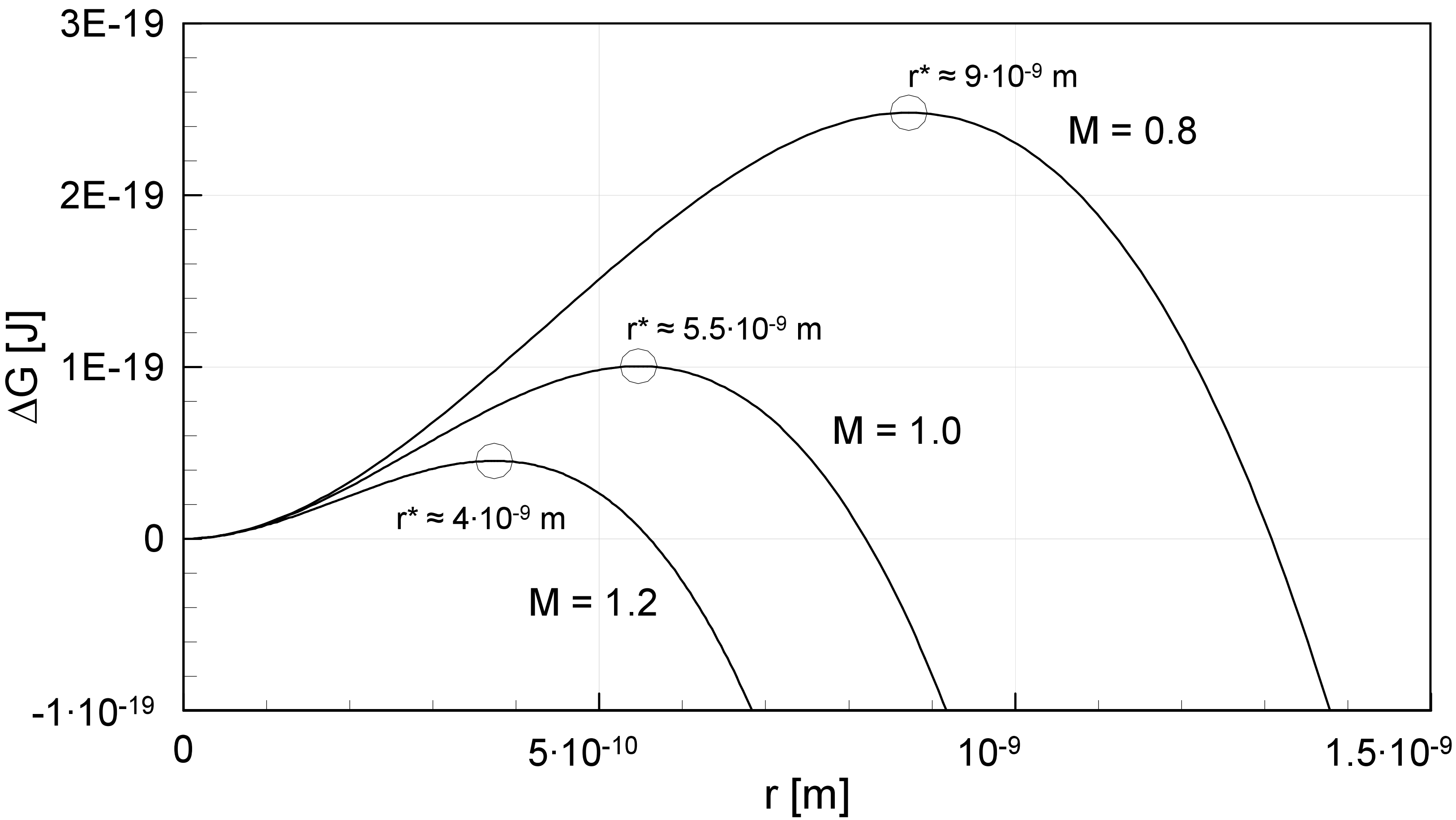

T_0 = 295 K

$p_0 = 10^5$ Pa

Φ_0 = 65 %

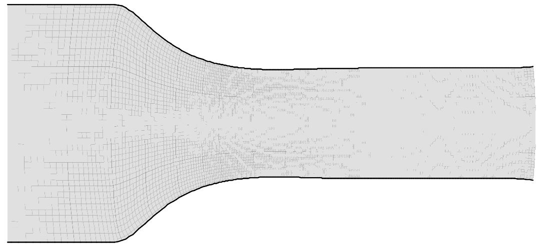

Transition in Nozzle A1

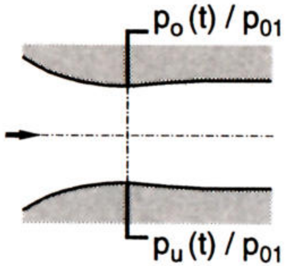

$$\Delta p(t) = \frac{p_o(t) - p_u(t)}{p_{01}}$$

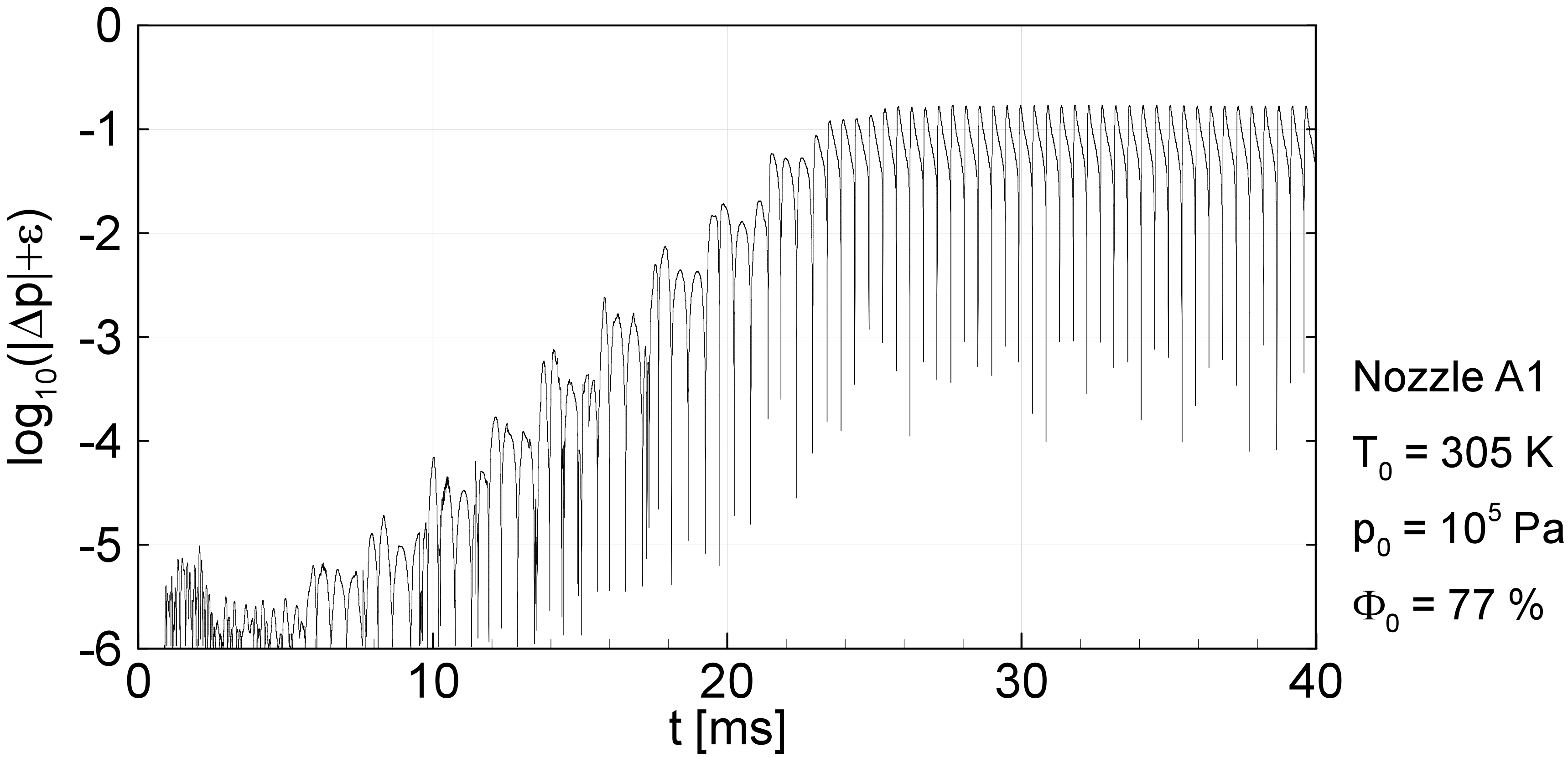

Transition in Nozzle S2

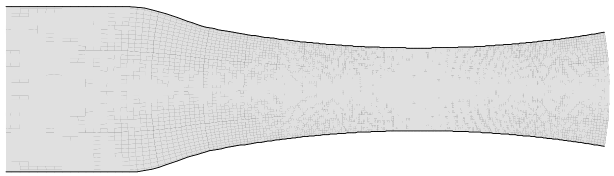

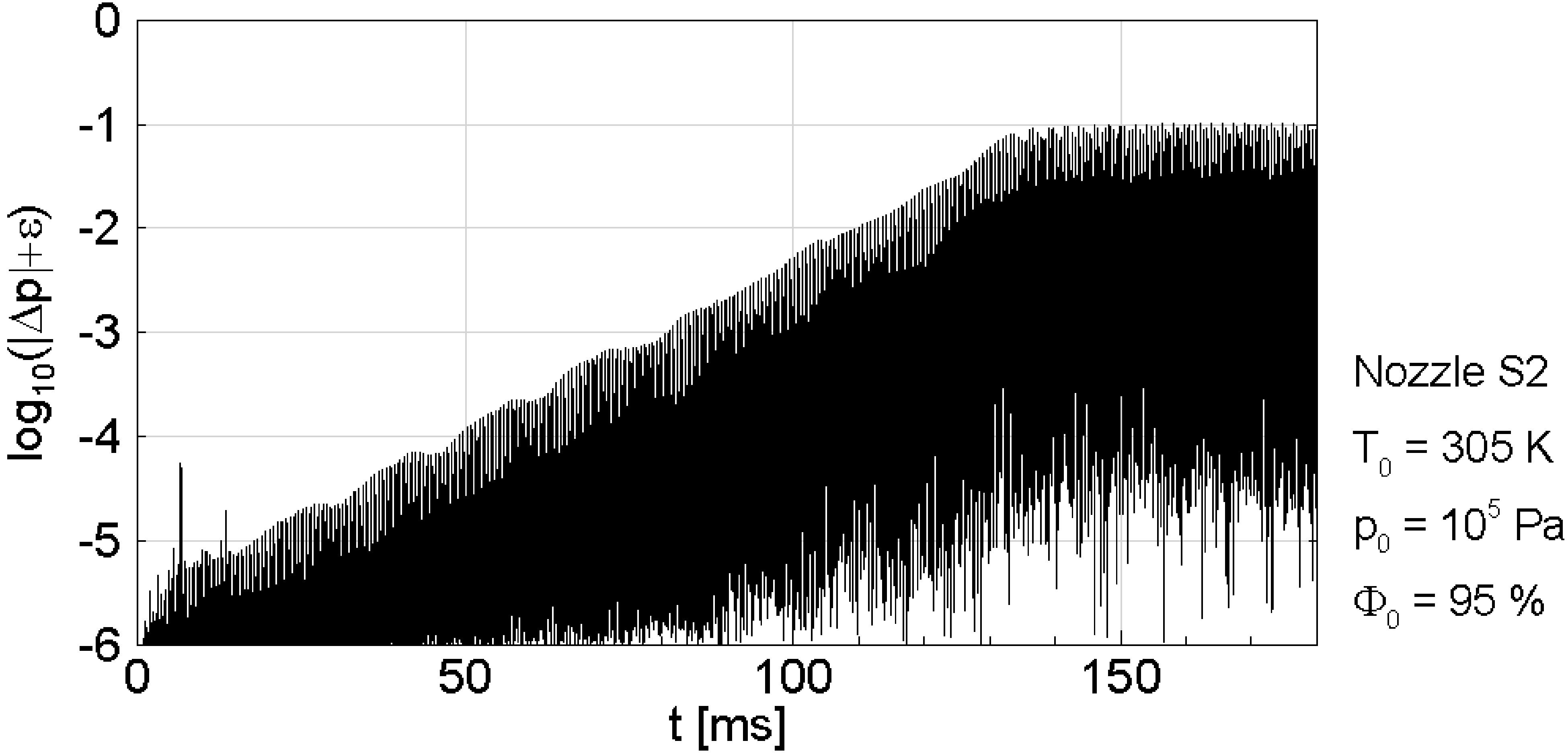

Appendix 1

Validation with Subcritical Flow in Nozzle S2

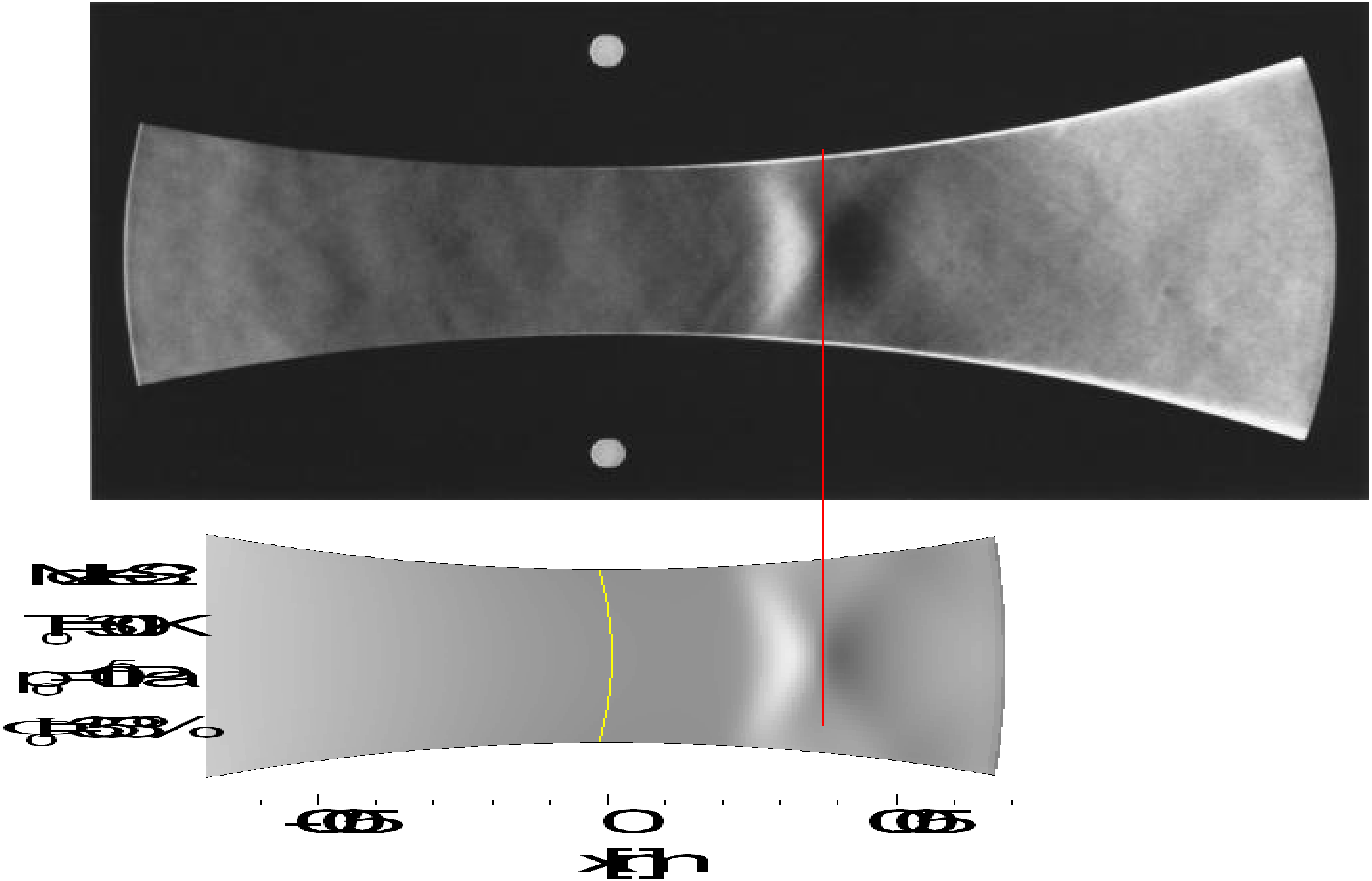

Heat Addition by Condensation

- latent heat L [kJ/kg] of gases in air:
  - H_2O: 2260
- specific heat capacity c_p [kJ/kg/K]:
  - air: 1.004
- Increase of static